Ship Detection With SAR C-Band Satellite Images: A Systematic Review

Cyprien Alexandre, Rodolphe Devillers, David Mouillot, Raphael Seguin, and Thibault Catry

***Abstract*—Detecting and tracking ships remotely is now required in a wide range of contexts, from military security to illegal immigration control, as well as the management of fisheries and marine protected areas. Among the available methods, radar remote sensing is increasingly used due to its advantages of being rarely affected by cloud cover and allowing image acquisition during both day and night. The growing availability over the past decade of free synthetic aperture radar (SAR) data, such as Sentinel-1 images, enabled the widespread use of C-band images for ship detection. There is, however, a broad range of SAR data processing methods proposed in the literature, challenging the selection of the most appropriate one for a given application. Here, we conducted a systematic review of the literature on ship detection methods using C-band SAR data from 2015 to 2022. The review shows a partition between traditional and deep learning (DL) methods. Earlier methods were mainly based on constant false alarm rate or polarimetry, which require limited computing resources but critically depend on ships' physical environment. Those approaches are gradually replaced by DL, due to the growth of computing capacities, the wide availability of SAR images, and the publication of DL training datasets. However, access to these computing capacities may not be easy for all users, which could become a major obstacle to their development. While both methods have the same objective, they differ both technically and in their approaches to the problem. Traditional methods mainly focus on ship size in spatial units (meters), whereas DL methods are mainly based on the number of ship pixels, regardless of image resolution. These latter methods can result in a lack of information on ship size and, therefore, a lack of knowledge that could be useful to specific applications, such as fisheries and protected area management.**

***Index Terms*—Maritime domain awareness, remote sensing, small ship, synthetic aperture radar (SAR), vessel detection.**

I. Introduction

THE characterization and monitoring of human activities at sea are of growing interest in various fields, such as maritime traffic [1], marine pollution monitoring [2], fisheries management [3], protected area management [4], [5], and border control [6], [7], [8]. These activities can involve ships of various sizes, tonnages, and shapes. Nowadays, maritime transportation represents more than 80% of goods transported worldwide [9], with more than 102 000 ships of 100 gross tons (GT) and above sailing across the globe in 2022. In accordance with several global, regional, and national regulations, certain ships (e.g., large ships or any ship carrying passengers) must be equipped with onboard GNSS transponders that transmit ships' positions in near real time. In the remainder of this article, "ship" refers to any large boat, mobile or not, transporting people or goods. The ability to accurately locate and characterize ships is the key to a variety of applications, ranging from safety and security to environmental monitoring and commercial activities [10]. Systems exist to help track ships' movements, including the automatic identification system (AIS), the long-range identification and tracking, and the vessel monitoring system used more specifically in fisheries enforcement [11], [12].

An AIS was initially designed for ship collision avoidance, environmental protection, and navigation efficiency [13]. It is now required on all ships over 500 GT and over 300 GT on international voyages, and those transporting more than 12 passengers [13]. Countries and intergovernmental organizations can also impose their own requirements. All European Union flagged fishing ships over 15 m in length and all commercial United States flagged fishing ships over 65 feet (about 20 m) in length are, for instance, required to be equipped with AIS [14], [15]. AIS information includes ships' identification, position, and type (among 16 classes) [13]. However, as AIS is not mandatory on all ships, it does not track most leisure ships and small fishing ships that are, therefore, not monitored within the framework of management plans. Some ships are also known to operate in the dark, turning OFF or altering their AIS signal [16]. Consequently, the use of the maritime domain remains partly unknown, with potentially many "not publicly tracked" ships or "dark fleets" imperiling our ability to manage and survey coastal areas that are the most critical for fisheries, security, human impact, and biodiversity conservation [17].

For this reason, systems such as AIS are often combined with other sensors when trying to assess maritime traffic and fishing efforts [18]. Satellite remote sensing has been increasingly used, both with optical and synthetic aperture radar (SAR) sensors, to improve ship detection at sea [19], [20], [21], [22]. Due to its higher spectral and often spatial resolutions, optical imagery is an efficient and complementary solution to SAR imagery for ship detection but is dependent on low cloud coverage, making

Manuscript received 27 March 2024; revised 24 May 2024 and 2 July 2024; accepted 21 July 2024. Date of publication 2 August 2024; date of current version 26 August 2024. This work was supported by the Région Occitanie, France, under the project DECOSAR under Project #21019812 (Recherche et Sociétés - 2021). *(Corresponding author: Cyprien Alexandre.)*

Cyprien Alexandre, Rodolphe Devillers, and Thibault Catry are with the French National Research Institute for Sustainable Development, Research Lab Espace-dev, 34093 Montpellier, France (e-mail: cyprien.alexandre@ird.fr; rodolphe.devillers@ird.fr; thibault.catry@ird.fr).

David Mouillot is with Research Lab MARBEC, University of Montpellier, 34095 Montpellier, France (e-mail: david.mouillot@umontpellier.fr).

Raphael Seguin is with the Research Lab MARBEC, University of Montpellier, 34095 Montpellier, France, and also with Bloom Association, 75010 Paris, France (e-mail: raphaelseguin@protonmail.com).

Digital Object Identifier 10.1109/JSTARS.2024.3437187

its application particularly challenging in tropical regions and during some seasons [20]. SAR remote sensing is an alternative to obtain images independently from weather conditions and at night time [23], [24], [25] but it can be challenging in terms of data processing. The noise present in SAR images, known as speckle, increases the average signal level in the image and can make distinguishing the signal from a ship difficult. If the speckle and the potential presence of false positives (rocks, wrecks, waves, and offshore infrastructures) can complicate automatic detection and identification of ships [26], the high contrast between the background water and the ships when using SAR images facilitates ships' detection and identification [27]. The increasing number of C-band SAR sensors, including RADARSAT-2 (RS2) launched in 2007, Sentinel-1 (S1) in 2014, Gaofen-3 (GF3) in 2016, and the RADARSAT Constellation Mission (RCM) in 2019, allows the massive and rapid acquisition of diverse SAR data that can be used for ship detection. Yet, the only C-band SAR sensor providing free images is S1 from the European Space Agency, making S1 an increasingly popular remote-sensing sensor for ship detection.

The automatic ship detection on SAR images remains challenging. Many data processing methods have been proposed to automatically identify ships from SAR images and have been broadly classified into two categories: traditional and deep learning (DL) based methods [28], [29]. Traditional methods are largely dominated by the constant false alarm rate (CFAR), a method that consists of modeling the water noise (i.e., clutter) using statistical models in order to separate features on the SAR image likely to be associated with ships from the rest. Clutter is a characteristic noise caused by the movement of water. It can cause a strong backscatter approaching that of a target and limiting its detection. The clutter effect can be mitigated by a robust clutter model in the case of traditional algorithms or, in the case of DL algorithms, by training data under a variety of conditions, including scenes with significant clutter (e.g., using the SAR-Ship-Dataset [30]).

Since the arrival of S1 and GF3, the amount of SAR data available has exploded, allowing the emergence of new data-intensive methods based on DL that are revolutionizing many research fields but require large datasets for training the algorithms [28]. For ship detection, many of these DL-training datasets are the result of cross-referencing SAR images with AIS information [31], [32], [33] or expert labeling of ships on images [30], [34]. While extensive literature is available on the topic, specific questions and challenges still need to be addressed. It can be difficult to know which method is more efficient or more appropriate for certain applications (e.g., ship size) or contexts (e.g., sea conditions). As SAR images from S1 play an increasing part in today's ship detection efforts, we focus on studies attempting to detect ships from C-band SAR images. This article presents a systematic review of the literature on the use of C-band SAR images for the detection of ships at sea. Systematic reviews are increasingly acknowledged as being the most robust approach to provide an unbiased overview of a given scientific field. We first describe the commonly used preferred reporting items for systematic reviews and meta-analyses (PRISMA) methodology used for this systematic review, presenting the databases, the keywords, and the years selected used for the review. After providing an overview of the field of ship detection, we present selected methods and data from our selection of articles. We then discuss the limitations of current detection methods and the reproducibility of the proposed methods to finally propose perspectives for this field.

II. Review Method

This study uses the PRISMA [35], which aims to enhance transparency in reporting systematic reviews by outlining the rationale, methods, and findings. In this section, we focus on the criteria and search engines, as well as the article selection workflow that was used to establish the final selection of articles.

A. Bibliographic Search Engine Selection

Six search engines were used for the literature review, with one specific to the field of computer sciences (ACM digital library) and five more interdisciplinary ones (IEEE, Scopus, Taylor and Francis, Wiley, and the Web of Science). The choice of search engines was informed by Gusenbauer and Haddaway [36], selecting them for their ability to handle queries using specific keywords and specific semantic elements, such as logical operators (e.g., AND, OR, NOT) and parentheses. We have also retained search engines listing "remote sensing" in their topics and have, for practical reasons, restricted our choice to search engines offering bulk downloads of the results.

B. Search Criteria

Four sets of search criteria were used in our review, helping select papers that mentioned SAR images, ship detection, and C-band sensors (e.g., S1). The final criterion aimed to exclude airborne sensors, hence restricting the search to satellite ones. The selected search criteria are built around logical operators to form the following search expression.

"(SAR OR "synthetic aperture radar") AND ("ship detection" OR "vessel detection" OR "ship identification" OR "vessel identification" OR "ship detector" OR "vessel detector") AND ("Sentinel-1" OR "RCM" OR "RADARSAT Constellation Mission" OR "Gaofen-3") NOT ("airborne" OR "aircraft")."

Among C-band SAR satellites, only S1 provides free data, making it key for some approaches. This is why the search was restricted to papers published since 2015, the first complete year of S1 SAR images release, to November 2022, when this review was carried out.

C. Final Selection

The search identified 1188 publications (e.g., journal papers and conference proceedings), from which 240 were duplicates that were excluded (see Fig. 1). Publications were further screened for their accessibility (incorrect DOI, papers not available), from reading their title and abstract, and finally following a review of the entire document. Papers not in the English language, with incorrect topics, not using C-Band sensors, or not discussing specific algorithms were excluded. This screening

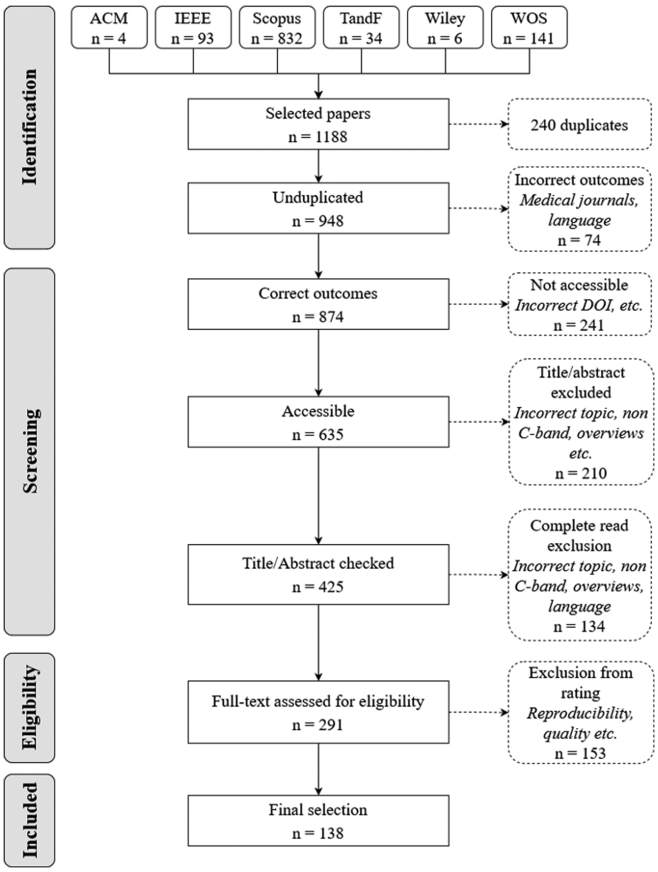

Fig. 1. PRISMA workflow presenting the selection process of articles about ship detection using C-band SAR imagery.

resulted in identifying 291 papers, including one book chapter, 88 conference papers, and 202 journal articles.

A three-point scoring system was established (3 being the best score) and applied to assess the overall relevance of the 291 publications. This scoring took into account the thoroughness of the method description and considered whether the data used by the publication were commercial or open-source. The maximum score was given to a publication whose code was shared and fully reproducible using free data. Papers with a score of 1 were excluded and the final selection included 138 papers, including 11 conference papers and 127 journal articles.

This final set of papers was analyzed using descriptive statistics and a co-occurrence graph to study the evolution and linkage of method types over the chosen period. Co-occurrence networks are nondirectional graphical representations of the use frequency of variables and the frequency with which they appear together. This co-occurrence network was produced using the R package Bibliometrix [37] and using the abstracts and keywords of the papers as input.

III. Results

A. Methods Used for Ship Detection

The final 138 publications used methods that could be classified into two main categories: traditional methods and DL-based methods (see Table I), each of them being composed of subcategories. Methods from each of these categories have advantages and limitations that are summarized in Table II. All SAR image detections share a common preprocessing step that includes image despeckling. By applying a filter, this step smoothes the noise generated by the sensor. As this step is common to all methods, it is not specifically described in the methods that follow.

1) Traditional Methods: CFAR is a technique commonly used in signal processing, particularly in radar systems, to detect targets against a background of noise (sea clutter, the radar echoes produced by the sea surface). The mathematical principles behind CFAR involve statistical hypothesis testing and adaptive thresholding. CFAR assumes that the background signal (or noise) follows a known statistical distribution. The most commonly used in the reviewed articles are Gamma [39], [44], [48], Log-normal [40], [53], and K-distributed models [11], [46], [47]. CFAR then uses adaptive thresholding, based on the local noise level and the use of concentric moving windows, to detect targets. The center window contains the cells under test (CUT), and therefore the possible targets. The furthest window from the CUT is the background window where the clutter statistics are computed. The intermediate guard window serves as a protection to prevent any leakage of target pixels into the background region. Statistics are calculated from neighboring cells or background samples. These statistics represent the noise level in the vicinity of the cell being tested for the presence of a target. CFAR employs statistical hypothesis testing to decide whether a signal in a cell corresponds to a target or is merely background noise with the objective to maintain a CFAR over varying background noise levels. This means that the probability of falsely detecting a target (false alarm) remains the same regardless of changes in noise intensity or environment. Different types of CFAR can be used for target detection. Two typical methods are cell-averaging CFAR (CA-CFAR) and two-parameter CFAR (2P-CFAR) [48]. CA-CFAR uses the mean of adjacent cells to estimate the clutter (1), while 2P-CFAR uses both the average and standard deviation of the adjacent cells

$$P_n = \frac{1}{N}\sum_{i=1}^{N} x_i \tag{1}$$

where P_n represents the estimated noise power, N is the number of training cells, and x_i is the sample in each training cell.

The main challenge with these methods lies in adapting the models to sea conditions, such as waves, that alter the statistical properties of pixels and hence impact the set thresholds [11]. A threshold set too low will result in more targets being detected at the cost of increased false alarms. Conversely, if the threshold is set too high, the number of nondetected targets will increase but the occurrence of false alarms will be reduced, risking to miss potential ships on the images.

Among all the articles using CFAR methods, the search for unidentified maritime objects (SUMO) algorithm [11] stands out with 17 citations among the articles selected for this review. SUMO models sea clutter using a K-distribution is available in open-access on GitHub [168] and can process SAR images

TABLE I
TYPOLOGY OF SHIP DETECTION METHODS

		Algorithm example	References
Traditional	CFAR-based	2P-CFAR, CA-CFAR	[11], [26], [38], [39], [40], [41], [42], [43], [44], [45], [46], [47], [48], [49], [50], [51], [52], [53]
	Polarimetry	Fusion, SVD	[7], [16], [54], [55], [56], [57], [58], [59], [60], [61], [62], [63], [64], [65]
	Others	HarrLike, Complex Signal Kurtosis, SVM	[66], [67], [68], [69], [70], [71], [72], [73]
Deep-learning based	Two-stage	Fast R-CNN, Faster R-CNN	[19], [22], [74], [75], [76], [77], [78], [79], [80], [81], [82], [83], [84], [85], [86], [87], [88], [89], [90], [91], [92], [93], [94], [95], [96], [97], [98], [99], [100], [101], [102], [103], [104], [105], [106], [107], [108], [109], [110], [111], [112], [113], [114], [115]
	One-stage anchor based	Yolo, SSD, RetinaNet	[20], [116], [117], [118], [119], [120], [121], [122], [123], [124], [125], [126], [127], [128], [129], [130], [131], [132], [133], [134], [135], [136], [137], [138], [139], [140], [141], [142], [143], [144], [145], [146], [147], [148], [149], [150], [151], [152], [153], [154], [155], [156]
	Anchor free	CenterNet, FCOS	[157], [158], [159], [160], [161], [162], [163], [164], [165], [166], [167]

TABLE II
ADVANTAGES AND LIMITATIONS OF SHIP DETECTION METHODS

		Advantages	Limitations
Traditional	CFAR	- Limited computing resource requirements - Can be associated with DL	- Highly environment-dependent - False alarms
	Polarimetry	- Increased contrast - More polarization information - Better detection rate than single-polarization	- Limited number of sensors and/or commercial - Can be time consuming
	Others	- Reduces false alarms	- Rarely used
Deep-learning based	Two-stage	- Good accuracy	- Slower than one-stage - High resource consumption
	One-stage anchor-based	- Faster than the two-stage	- Speed dependent on number of anchors - Less accurate
	Anchor-free	- Among the fastest DL methods	- Less explored for ship detection

from different sensors and different wavelengths, such as S1, RS2, TerraSAR-X (TSX), TandemX (TDX), and ALOS2.

We found other CFAR methods developed to increase the detection rate and limit false alarms. Lin et al. [38] added a variance correction term to the log-logistic model to improve CFAR ship detection under a complex background. This method could reduce false alarms by 20% when compared with a conventional log-logistic model.

Tian et al. [41] proposed a two-stage kernel density estimation CFAR. The first step is a prescreening with a global threshold, followed by a local threshold based on a moving window. Compared with a traditional CFAR with K-distribution, the authors obtained a rise of 8% in the detection rate and a drop of 4% in the false alarm rate. Calculation time was also reduced by more than 60%.

Ji et al. [42] proposed a variability index and excision CFAR (VIE-CFAR) function of the signal's mean and variance. VIE-CFAR achieved better results than CA-CFAR both in terms of the number of detected ships and the number of false alarms.

Zhang et al. [44] proposed a CFAR method for superpixel segmentation with a Gamma distribution of clutter. In contrast to a CFAR method with a moving window, the authors chose to model the clutter as close as possible to the target pixels for better clutter estimation and to avoid window computation time. This method achieves better results than other CFAR methods and considerably reduces calculation times.

Leng et al. [47] proposed a CFAR method based on a K-distributed model, with different calculations of clutter statistics depending on image resolution. For low-resolution images (>3 m), the clutter is modeled on a reference window, such as

a conventional CFAR. For high-resolution images, the clutter is modeled using pixels located on the edges of the images that have been cut into 512×512 pixel thumbnails. This method aims to reduce computing time on high-resolution images, such as TSX.

Ai et al. [53] proposed a bilateral-trimmed-statistics-based CFAR (BTS-RCFAR) based on a 2P-CFAR that uses a log-normal distribution. BTS-RCFAR uses two-sided adaptive thresholding to eliminate high- and low-intensity outliers and obtain a pure clutter sample. BTSR-CFAR obtains better results in terms of detection rate and false alarms than classical CA-CFAR and 2P-CFAR but is more time consuming.

Polarimetric synthetic aperture radar (PolSAR): The general mathematical principles of using PolSAR for target detection involve the understanding of polarization diversity, the analysis of scattering matrices, the statistical characterization of polarimetric signatures, and the application of specialized algorithms for target detection in radar imagery. PolSAR uses the polarimetric properties of the SAR signal to characterize the scattering behavior of different objects. This method uses the four possible vertical (V) and horizontal (H) polarization modes (i.e., VV, VH, HV, and HH) to model the interactions between detected objects and scattering [169]. In PolSAR, the scattering properties of targets are characterized by the complex scattering matrix. This matrix describes how incident radar waves are scattered in different polarization channels after interacting with the target. Targets show specific polarimetric signatures (due to their shape, orientation, and material properties), which are filtered using polarimetric decomposition models (e.g., Freeman–Durden decomposition, Cloude–Pottier decomposition) to analyze statistically and interpret PolSAR signal by breaking down the total backscattered signal into different scattering mechanisms, such as surface scattering, double-bounce scattering, and volume scattering. Yet, PolSAR is limited in its use by the type of sensor, which must transmit and receive waves in all four polarization modes. Only C-band commercial SAR images from RS2, RMC, and GF3 are fully polarized, offering a limited choice of data compared to other methods. Some authors compared their results with other methods based on CFAR and simple polarization.

Mahgoun et al. [55] used RS2 SAR images to compare CA-CFAR, 2P-CFAR, and the generalized likelihood ratio test methods. It demonstrates that CA-CFAR, when associated with singular value decomposition (SVD), achieves better results than CA-CFAR with single polarization or fusion. In the best case, CA-CFAR with SVD achieves a detection probability of 91% for a false alarm of 0.05%.

Zhang et al. [56] used a covariance matrix prior to span (summation of the three polarimetric intensity channels) and compared this method to 2P-CFAR. The method achieves better detection results but the calculation time can be 160 times longer than 2P-CFAR when the image size is large (1465×1940 pixels).

Marino and Hajnsek [61] used the geometrical perturbation-polarimetric notch filter on RS2 SAR images. Authors showed that polarimetric data are particularly beneficial when the detection is aimed at small or fast-moving targets in high sea clutter compared to a single-channel detector.

Other traditional methods are mentioned in the literature but are less common. Schwegmann et al. [66] used Haar-like feature extractions after initial zone identification (prescreening) using the CA-CFAR method. The Haar-like classifier is used to eliminate persistent false alarms from the CFAR method, resulting in a detection accuracy of 89%. However, this method computes a large number of features, which may result in long computation times.

Two articles used support vector machine (SVM) classifiers in their ship detection method. Li et al. [54] used an SVM classifier on rotation domain features from polarimetric RS2 and GF3 data. He et al. [67] used an SVM classifier on a gray-level co-occurrence matrix from S1 SAR images and reported increased accuracy and reduced false alarms compared to a CFAR method.

Proença and Marques [68] proposed a wavelet-based method that is faster than SUMO but needs to be tested on larger datasets. Leng et al. [69] used complex signal kurtosis (CSK) to detect ships. This method takes advantage of the non-Gaussian nature of the model to best discriminate clutter and ships, even in difficult conditions. This method considerably reduces false alarms caused by radio frequency interferences (RFIs).

While these methods offer improvements in accuracy over the CFAR, they are less frequently used in the literature. As the studies were carried out under conditions specific to each article, it is difficult to assert whether these methods would offer better results in other contexts.

2) Deep Learning-Based Methods: Existing reviews have been published specifically on DL ship detection methods (see [12], [28], and [29]), offering detailed taxonomies of algorithms. We will hence cover those methods more rapidly. Object detection methods based on DL fall into three main categories (defined in the literature cited above): two-stage detector, one-stage anchor-based, and anchor-free (see Fig. 2).

Two-stage approaches are based on the principle of "region proposal," where the image to analyze is not fed directly to the detector. Instead, the first stage splits the image into regions that could contain the object to be detected before proceeding to the rest of the analysis. Fast R-convolutional neural network (R-CNN) and faster R-CNN are prime examples of two-stage approaches [76], [82], [83]. Other studies use traditional methods, such as CFAR, as region proposal [26], [71] before conducting the detection stage using a CNN. Two-stage approaches are generally considered slower but more accurate than one-stage ones [28].

One-stage anchor-based approaches use anchors—bounding box (bbox) rectangles—initialized on each image cell. As soon as an anchor box is identified as containing part of the object to be detected, it is aggregated with its neighbor, which is also identified as containing part of the object, until it contains the entire object. Several boxes, of different shapes and sizes, can be initialized to increase the accuracy of the algorithm, with a potential negative effect on inference time. The YOLO series is a good example of such an approach [149], [150], [153]. Anchor-based methods are faster than two-stage ones but sensitive to hyperparameters, such as bbox size and ratio, and to the accuracy of training set bboxes.

Anchor-free methods are designed to be similar to human vision and do not initialize anchors prior to detection. They can directly predict key points relative to the object (center or top-left

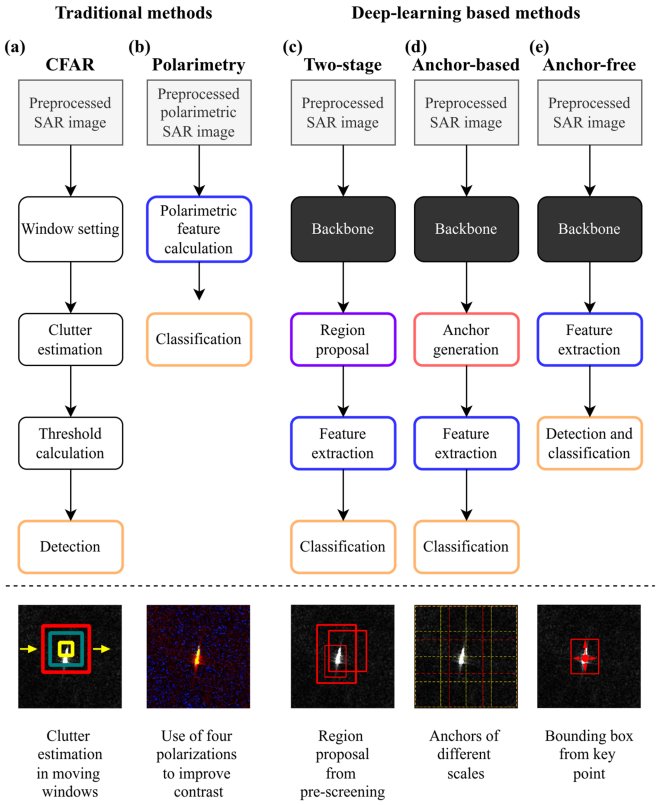

Fig. 2. Overview of key steps of different ship detection methods. (a) CFAR. (b) Polarimetry. (c) Two-stage. (d) Anchor-based. (e) Anchor-free.

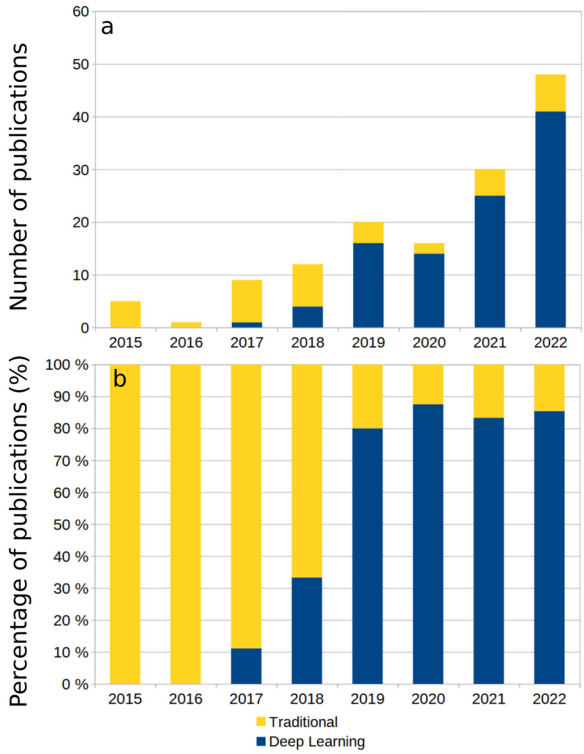

Fig. 3. (a) Number and (b) proportion of publications reviewed dealing with traditional or DL methods to detection ships per year.

bottom-right) before delineating the bbox containing the object detected [157], [162], [170]. This approach can be particularly useful for ship detection when ships are sparsely distributed in the image. With this method, there is no need to create multiple anchors where there are no ships. Although this technique is faster, it is relatively new and has not yet been widely used for ship detection.

3) Evaluation Metrics: In order to better understand the results described in the papers referred to in Section III-B, we describe common metrics used to evaluate the algorithms encountered in this review as follows:.

$$\text{Accuracy} = \frac{\text{TP} + \text{TN}}{\text{TP} + \text{TN} + \text{FP} + \text{FN}} \times 100\% \quad (2)$$

$$\text{Precision} = \frac{\text{TP}}{\text{TP} + \text{FP}} \quad (3)$$

$$\text{Recall} = \frac{\text{TP}}{\text{TP} + \text{FN}} \quad (4)$$

$$F1 - \text{Score} = 2 \times \frac{\text{Precision} \times \text{Recall}}{\text{Precision} + \text{Recall}} \quad (5)$$

where TP is the number of true positives (ships detected), TN is the number of true negatives (ship absences detected), FP is the number of false positives (wrong ship detections), and FN is the number of false negatives (ships missed).

Accuracy represents the proportion of correctly classified objects out of the total number of samples. Precision measures the accuracy of positive predictions. Recall, also called sensitivity, measures the ability of the model to capture all positive instances.

F1-Score provides a balanced measure of a model's performance, considering both false positives and false negatives.

4) Global Trends in Ship Detection Methods: Since 2015, there has been a rapid increase in the number of articles dealing with ship detection using C-band SAR imagery, suggesting a strong research interest in this topic [see Fig. 3(a)]. We observe two major increases in the proportion of DL-based articles, in 2017 and 2019, that could be related to the publication of the now widely used SAR ship detection dataset (SSDD) [171] in 2017 [based on Sentinel-1 full-capacity (2016) and GF3 SAR images (2016)], and the publication of SAR-Ship dataset [30] in 2019.

Used in nearly 90% of all studies in recent years, DL-based algorithms largely dominate today's publications in the field of ship detection using SAR imagery. This can be seen in Fig. 3(b) but also in the terminology used in publications. The co-occurrence graph based on abstract and keywords (see Fig. 4) shows a clustering into four groups of the vocabulary used in the studies, and the importance of the links between them, materialized by the thickness of the lines. The DL (red) and traditional methods (green) are organized around the generic ship detection terms (blue).

DL-related terms include "data," "feature," "network," and the frequently recurring "SSDD" dataset. This part of the graph occupies the largest space, showing once again the prominence of these methods in our selection of articles.

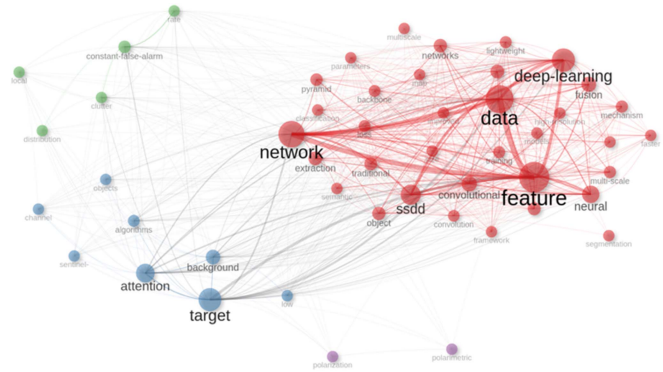

Fig. 4. Co-occurrence network of words from the papers' abstracts and keywords created using Bibliometrix [37]. The size of the circles indicates the frequency of words used and the lines' thickness indicates the frequency of terms used together. The DL (red) and traditional methods (green) are organized around the generic ship detection terms (blue). Purple refers to polarimetry.

Traditional methods (green) are characterized by terms such as "CFAR," "clutter," or "distribution." Although technically opposed, there are weak relationships in the graph, materialized by fine links between traditional and DL methods that point to the fact that some DL methods use traditional algorithms as region proposals, to prescreen SAR.

Articles related to polarimetry are distinguished by terms such as "polarization" or "polarimetric" (purple). These terms are limited in number and are relatively distinct from other methodologies, with minimal connections to the other approaches.

B. Ship Size

The size of detected objects is a crucial element when evaluating the detection capacities of algorithms that have not been discussed in other reviews in the field. In this section, we will analyze the representation of ship size in data and detection algorithms through the prism of both traditional and DL methods.

1) Ship Size in Data: Three types of data are used in the papers reviewed: 1) unmodified SAR images, as provided by the sensors and processed for use; 2) portions of SAR images contained in datasets created to train and test the DL algorithms, often in the form of annotated SAR thumbnails—some containing ship size information from AIS data; and 3) AIS data, the "ground truth" used to build datasets or validate the output of detection algorithms. This is generally the source of information for the size of detected ships.

Traditional methods generally combine SAR with AIS data at the validation stage. In articles using traditional methods, free SAR images are the most widely used, with S1 present in 50% of articles (see Fig. 5). In orbit from 2007 to 2017, RS2 has the longest operating life of any sensor used for traditional ship detection methods. Almost half of the reviewed articles used RS2 data.

In total, 12 training datasets were identified in the reviewed papers with DL methods (see Table III). All datasets contain C-band SAR images and some also add X-band data, offering a finer spatial resolution. The most widely used dataset is SSDD (see Fig. 6), composed of RS2, TSX, and S1 SAR images,

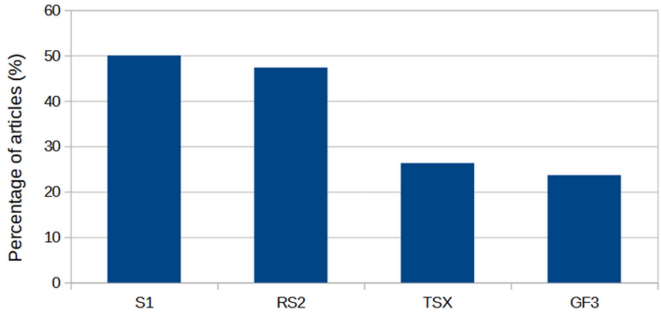

Fig. 5. Proportion of articles using the four most used SAR sensors in traditional methods.

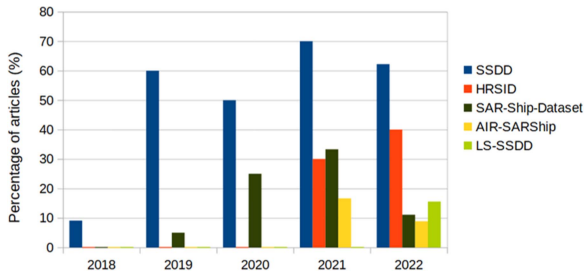

Fig. 6. Proportion of articles using the five most used datasets per year.

published in 2017. Other datasets were derived from SSDD and specialized by the sensor (e.g., Gaofen-SSDD, Sentinel-SSDD) or for small-sized ships (e.g., Large-Scale-SSDD, LS-SSDD).

Image labeling can take the form of polygons for segmentation, bounding boxes, or rotated bounding boxes. Rotated bounding boxes can provide an approximation of the observed ship size on the SAR image. They are mostly annotated by experts who directly label the SAR images, sometimes with the help of additional optical images [30], [75], [171], [172], [173], [174]. LS-SSDD [33] uses AIS as a ship position ground truth for labeling. OpenSARShip-1.0 and 2.0 [31], [32] are the only two datasets that use AIS data to annotate ship sizes, showing their length, width, and AIS category. Despite this, these datasets are only used in three articles selected in our review and do not appear in the five most frequently used datasets (see Fig. 6).

Although these datasets are mainly used in DL, three traditional algorithms use AIR-SARShip, LS-SSDD, and high-resolution SAR images dataset (HRSID) or SSDD [39], [48], [43] with no more information on size than that given in the dataset.

The HRSID [173] and dual-polarimetric SAR ship detection dataset (DSSDD) [174] both align with the Microsoft COCO nomenclature, a standard dataset for generic object detection [167]. Datasets use 1024 pixels as the maximum size of a small object, based on images whose resolutions range from 3 to 10 m (i.e., TSX, TDX, and S1 SAR images). As a result, objects of identical size for the DL algorithm (same number of pixels) could have very different sizes (in meters).

The authors of LS-SSDD [33] define their dataset as specifically designed for small-ship detection under large-scale backgrounds. LS-SSDD defines the size of detected objects in

TABLE III
DL DATASETS USED IN SELECTED ARTICLES

	Date	Sensors	Locations	Scenes	Polarization	Resolution (m)	Ship classes	Ref
SSDD	2017	RS2, TSX, S1	China, India	Inshore, offshore	VV, VH, HH, HV	1 to 15	-	[171]
OpenSARShip-1.0	2017	S1	China, Singapore, Japan, UK	-	VV, VH	2.7 × 22 to 3.6 × 22, 20 × 22	16 AIS types	[31]
OpenSARShip-2.0	2017	S1	China, Singapore, Japan, UK	-	VV, VH	2.7 × 22, 3.6 × 22, 20 × 22	16 AIS types	[32]
AIR-SARShip-1.0	2019	GF3	-	Ports, islands, reefs, sea	Single	1, 3	-	[172]
SAR-Ship-Dataset	2019	102 GF3, 108 S1	-	Complex background	VV, VH, HH, HV	3, 5, 8, 10, 25, 1.7 × 4.3 to 3.6 × 4.9, 20 × 22	-	[30]
HRSID	2020	S1-B, TSX, TDX	World	Inshore, offshore	VV, HH, HV	0.5 – 3	-	[173]
LS-SSDD	2020	S1	Tokyo, Adriatic Sea + 13 other	Inshore, offshore	VV, VH	5 × 20	-	[33]
Sentinel-SSDD	2020	S1	South Korea, Japan	Inshore, offshore	VV, VH, HH, HV	-	-	[75]
Gaofen-SSDD	2020	GF3	China	Inshore, offshore	VV, VH, HH, HV	-	-	[75]
DSSDD (dual polarimetric)	2021	S1	World	Inshore, offshore	VV+VH	2.3 × 14.0	-	[174]
SRSDD-v1.0	2021	GF3	China, Japan	Inshore, offshore	VV, HH	1	Ore–oil ships; Bulk cargo ships; Fishing boats; Law enforcement; Dredger ships; Container ships	[176]
SMCDD	2022	HISEA-1	-	-	VV, VH, HH, HV	1, 3, 10	Bridges; Ships; Oil tanks; Aircraft	[101]

proportion to the total size of the image. For example, according to the COCO definition, a small object is defined as being less than 1024 pixels in size on 484 × 578 pixels images, i.e., under 0.37% of the image. Hence, regardless of the image spatial resolution, a ship covering less than 0.37% of the image can be considered small.

2) Ship Size in Detection Algorithms: Only two publications using traditional methods discussed ship size in their results. Park et al. [49] used a CFAR method following a normal distribution on S1 SAR images and compared the results with the ship AIS positions in the area. The authors call "probability of detection" (POD) the percentage of ships successfully detected. The authors show the relationship between the image resolution and the POD, with PODs around 80% for ship sizes under 20 m that rise to 94% for ships from 30 to 150 m.

Pelich et al. [16] used the nonnormalized coherence between VV and VH polarizations of S1 SAR images with a CFAR algorithm. The authors used AIS data to extract ships' sizes and evaluate their detection rate. They argued that coherence does not provide additional precision in terms of detection rate compared to VV polarization, which itself gives a lower detection rate than VH. They considered that the detection rate is high for ships longer than 60 m (>80%) but drops sharply to 40% for smaller ships.

Other authors use ship size only as an input parameter for detection algorithms. Schwegmann et al. [66] used a modified Otsu's method for which a minimum and a maximum ship size parameter in pixels (set at 2 and 20, respectively) must be defined to determine the algorithm's window size. Other authors [41], [48] simply adjust the window size according to the size of the ships, without going into further detail.

Lanz et al. [7] go further and try to detect ships smaller than 15 m. The method presented is based on TSX and S1 polarimetry and deals with the detection of 12 m × 3.5 m × 0.5 m (length/width/height) rubber inflatables. This method is experimental but concludes that detection of very small nonmetallic craft, such as inflatable refugee ships, is possible with high-resolution SAR data and calm sea conditions.

In the DL field, improving the accuracy of ship detection algorithms involves better detection of small objects, i.e., representing few pixels, and therefore operating at multiple scales in the image. The main method used to detect ships at multiple scales is the feature pyramid network (FPN), introduced by Lin et al. [175]. FPN is regularly encountered [74], [76], [91], [93], [97] to detect small objects. It is composed of both a bottom–up and a top–down pathway. The bottom-up pathway is a classical CNN for feature extraction and the top–down one constructs higher resolution layers from a semantic rich layer. Higher level features are exploited for detecting larger objects, and lower level features are exploited for detecting smaller objects.

Almost all papers based on DL algorithms mention the size of objects to be detected but do it very briefly. Few define the size of ships and even fewer include it in their results. By default, the

size of an object is defined by the dimensions of its bounding box (horizontal or rotated) in pixels.

Dechesne et al. [95] aimed at classifying detected ships and predicting their length in meters. They collected AIS data corresponding to five ship classes: tanker, cargo, fishing, passenger, and tug. In addition to the standard metrics used in DL, they compared the size prediction error for two models: a multilayer perceptron (MLP) and a multitask architecture with three branches for detection, classification, and length estimation of ships.

After an initial test on data from European seas, they considered the MLP inaccurate for ship length estimation. Ship length was underestimated, with a very large standard deviation (mean error: -7.5 m $\pm$ 128 m). Their method achieved better results as length was slightly overestimated, with a mean error of 4.65 m $\pm$ 8.55 m for a four-class model, and a mean error of 1.93 m $\pm$ 8.8 m and an F-score of 97.4% for a five-class model.

After conducting tests with the OpenSARShip dataset, the authors observed that their method was dependent on the training dataset. The difference in materials used for ships between European and Asian waters could have impacted the algorithm capabilities.

All other authors used pixel units to define ship size. The number of pixels can refer to a horizontal bounding box, a rotated bounding box, or a polygon extracted from segmentation. Chen et al. [93] used FPN to detect small targets defined "with a scale below 64 pixels." Jiang et al. [136] referred to the size of the SSDD bounding box.

Su et al. [100] created SII-Net, a two-stage algorithm specifically developed for small target detection and trained with LS-SSDD. They concluded with an improvement in the detection of small ships compared with existing algorithms, particularly on small targets, which they define as smaller than 30×30 pixels. However, the detection accuracy of ships smaller than 400 pixels remains objectively low compared with larger ships.

Chen et al. [121] attempted to improve the accuracy of their algorithm through better detection of small ships by focusing on anchor boxes. With a multiscale adaptive recalibration network, authors used an FPN to propose anchor box sizes adapted to the detected object. They also introduced the notion of a rotated bounding box to limit the proportion of background signal in the total bounding box signature compared to a horizontal bounding box. Rotated bounding boxes are also more appropriate for estimating ship size.

IV. Discussion

We conducted a systematic review of the literature on ship detection using C-band SAR. The free Sentinel-1 images are essential for radar remote sensing, particularly for ship detection. We, therefore, thought it useful to use the characteristics of these SAR images as a criterion for our review. This review has provided us with an overview of the ship detection field, using both traditional and DL methods. It has also led us to reach new conclusions, not covered in other, often DL-oriented, reviews. The study of 138 articles shows a trend over time in the types of methods used. Ship detection research has been in constant evolution since 2015 with a rapid increase in the number of publications and a recent shift toward the use of DL algorithms. Beyond the increasing computing capacity, the volume of available data has supported the growth of DL in the field of ship detection. The large amount of data required to train DL algorithms has long been an obstacle to the use of such methods. The free availability of S1 data at the end of 2014 and the publication of the first SSDD dataset in 2017 were key elements in the development of these techniques. Later, the publication of more specialized datasets and the launch of GF3 also helped boost publications in this field. It sometimes seems complicated to access large computing capacities (cost, knowledge), such as high-performance computing centers. There is a desire to reduce the size of DL models, which could be run more easily on personal machines with GPUs or for on-board solutions [141], [148].

The shift toward the use of DL algorithms is, however, not complete, and publications using traditional methods still account for a proportion of the papers in recent years. While DL methods prove very effective, CFAR algorithms can offer convincing results with reduced computation times without the need for GPUs, often being sufficient to answer the objectives of some studies.

Recent studies such as [1] combined CFAR and DL for the detection and classification of global maritime traffic, suggesting that both approaches may in fact be complementary in some contexts. Those authors used a CFAR detection algorithm to extract ships from S1 data and analyzed those results with DL networks to filter out false detections (accuracy = 97.5%), classify fishing versus nonfishing ships (accuracy = 90.5%), and estimate ships' size (RMSE = 21.9 m). Combining the two approaches has the advantage of limiting false positives when compared to using CFAR alone. The DL classification algorithm acts as a filter for CFAR detections. The use of traditional methods reduces the number of zones where ships are potentially present and can be detected by DL models, thus improving ship detection performance and accuracy.

A key issue that emerged from the review is the definition of ship size. This notion has not been encountered by the authors in other review studies in the domain and is important in many fields, due amongst other reasons to the role ship size plays in diverse regulations governing the oceans. For instance, ships above specific sizes may not be allowed to operate in specific zones or could only be allowed at certain times. Data on ship size derived from SAR images are then potentially useful to monitor the level of compliance with regulations. Improving the accuracy of ship detection algorithms means improving the detection of challenging targets, such as small ships. It, therefore, seems essential to define the concept of "small" ship if we are to evaluate algorithms detecting them. In the literature, there is a notable difference in the approach to ship size used by articles using traditional and DL methods. While studies presenting traditional algorithms tend to focus on geographic concepts for distances, articles using DL-based algorithms seem more focused on computer science concepts of image resolution and the technical challenges of feature identification. As a consequence, while studies using traditional methods report ships' size in meters, DL studies report them as an absolute number of pixels, or as a proportion of pixels in the image. Data used in the

DL field are often derived from large datasets, incorporating SAR images from several sensors of various resolutions. In DL, as size is defined in pixels, the same object observed by sensors of different resolutions will not have the same size. The size of a given object can also vary depending on the labeling method used. The MS COCO standard specifies that an object, to be small, should be less than 1024 pixels in size. In a horizontal bounding box, the ship will represent only a part of these 1024 pixels. Depending on its orientation, it will also occupy more or less pixels of the bounding box. Oriented bounding boxes, or even segmentations, can be used to get closer to the real size of the object in pixels. Thus, for a given object size, the actual size occupied in pixels will be: Segmented $>$ Oriented BBox $>$ Horizontal BBox. The reviewed DL algorithms are unable to differentiate input image resolutions. If size is defined as the pixel count, discriminating ship sizes is hence impossible. This type of algorithm cannot be used, for example, to restrict access to a certain type of ship in a given area. To estimate the approximate size of the boats detected, SAR images of the same resolution should be used for training and inference.

Depending on the users' needs, traditional or DL algorithms can be used. Traditional methods are best suited to data processing using desktop machines and a limited number of images. In terms of detection, according to the results obtained by Pelich et al. [16] and Park et al. [49], detected ships should be at least three to six times the image resolution to obtain satisfactory POD (i.e., $>$ 80%). In the DL field, only one reviewed study discusses the physical size of detected ships [95], with highly variable results depending on the dataset used. In a study published after the reviewed period, Paolo et al. [1] reported slightly better results with S1 data, detecting 95% of ships over 50 m and 80% of ships between 25 m and 50 m in length, as long as ships are at least 1 km apart.

Detection capabilities as a function of size must be modulated according to other parameters. Several factors such as sensor parameters (e.g., angle, polarization), the ship environment (e.g., wind, clutter, inshore versus offshore), and the characteristics of the ships themselves (e.g., size, materials) can impact detection capabilities. Lanz et al. [7], who deal with the detection of inflatable rafts, indicated that the spectral signature of nonmetallic, fiberglass, or wooden ships will be lower for an equivalent size. Thus, according to Greidanus et al. [11], it is difficult to specify a minimum detectable ship size. Large nonmetallic ships can have a very low radar echo, while much smaller objects than the image resolution can be easily detected, such as small ships equipped with radar reflectors.

Generally, it remains challenging to reliably compare the accuracy of ship detection algorithms whether using traditional or DL methods. Detection and false alarm rates strongly depend on ground truth information that remains limited. AIS data and expert assessments may on their own be limited to assess false alarms. In DL, this false alarm rate can be limited by training using diverse data, including images without ships. Yet, all stationary objects that can create false positives can be removed from analyses [177]. In this regard, it would be interesting to systematically compare traditional methods with DL methods for ship detection and size estimation. To achieve this, the use of a metric from the international measurement system as a result standard seems essential.

Our study suggests that S1 SAR images are unavoidable for today's large ship detection projects, offering large volumes of free data dating back to 2015 for the entire planet. Such an offer should increase with the expected addition of the additional S1C and S1D satellites into the S1 constellation in 2024 and 2025. Moreover, these data are the most frequently used among the reviewed articles, making them both easily exploitable through open-source datasets and usable as input data for numerous algorithms presented in the literature. If the spatial resolution of S1 SAR images generally remains too low in applications such as the detection of ships of less than 15 m in length, other commercial solutions with a high revisit capacity exist in X-band (TSX, CAPELA, and ICEEYE) and could make it possible to detect smaller objects.

Our systematic review uses criteria related to the use of free and widely available data, i.e., Sentinel-1 SAR images. However, it should be noted that ship detection is part of the wider research on object detection. Within this framework, which is not the main topic of our study, we can observe works that are close to our subject, either in terms of theme or in terms of the detection methods used. In this common field of marine object detection, we can mention, for example, oil spill detection using DL or traditional algorithms [2], [175]. Conversely, more generic algorithms, or those from other fields with similar methods, could be used for boat detection, such as segmentation methods or MLP [179], [180].

Given the unprecedented expansion of the ocean economy leading to rapid growth of industrialization fishing, a global overcrowding of main maritime routes, and severe environmental degradation, our ability to monitor accurately anthropogenic activities at sea (both offshore and close to the coasts) is of crucial importance. For instance, the positions of about three-quarters of the world's industrial fishing ships are not publicly disclosed and can only be detected using remote sensing technologies [1]. This "dark fleet" may threaten vulnerable species even inside marine protected areas [181]. Therefore, with the goal to protect at least 30% of the ocean before 2030 for biodiversity, food, and climate [182], we urgently need better monitoring systems at high temporal frequency. Toward this objective, the coupling between high-resolution satellite imagery and the most efficient ship detection algorithms could be a major step forward [173]. Yet, despite the multiplication of sensors with a large variety of technical capacities, satellite imagery still fails to fill some gaps in ship detection and monitoring. Ship detection using high resolution SAR imagery has still the potential to improve our understanding of the dynamics of anthropic activities in the oceans, both in time and space, throughout the year, independently from weather conditions. The S1 constellation offers the capability of acquiring SAR images at different times of the day, covering a broad range of anthropic activities at sea [171], and an overview of maritime traffic over large areas. Satellite imagery shows us what would otherwise remain unseen: a quarter of transport and energy vessel activity and three-quarters of all industrial fishing vessels are not publicly tracked [170].

REFERENCES

[1] F. Paolo et al., "Satellite mapping reveals extensive industrial activity at sea," *Nature*, vol. 625, no. 7993, pp. 85–91, Jan. 2024, doi: 10.1038/s41586-023-06825-8.

[2] N. Aghaei, G. Akbarizadeh, and A. Kosarian, "Osdes_net: Oil spill detection based on efficient_shuffle network using synthetic aperture radar imagery," *Geocarto Int.*, vol. 37, no. 26, pp. 13539–13560, Dec. 2022, doi: 10.1080/10106049.2022.2082545.

[3] V. Klemas, "Fisheries applications of remote sensing: An overview," *Fisheries Res.*, vol. 148, pp. 124–136, Nov. 2013, doi: 10.1016/j.fishres.2012.02.027.

[4] S. Cope, B. Tougher, J. Morten, C. Pukini, and V. Zetterlind, "Coastal radar as a tool for continuous and fine-scale monitoring of vessel activities of interest in the vicinity of marine protected areas," *PLoS ONE*, vol. 17, no. 7, Jul. 2022, Art. no. e0269490, doi: 10.1371/journal.pone.0269490.

[5] T. Appleby, M. Studley, B. Moorhouse, J. Brown, C. Staddon, and E. Bean, "Sea of possibilities: Old and new uses of remote sensing data for the enforcement of the ascension Island marine protected area," *Mar. Policy*, vol. 127, May 2021, Art. no. 103184, doi: 10.1016/j.marpol.2018.06.012.

[6] U. Kanjir, "Detecting migrant vessels in the Mediterranean Sea: Using Sentinel-2 images to aid humanitarian actions," *Acta Astronautica*, vol. 155, pp. 45–50, Feb. 2019, doi: 10.1016/j.actaastro.2018.11.012.

[7] P. Lanz, A. Marino, T. Brinkhoff, F. Koster, and M. Moller, "The InflateSAR campaign: Testing SAR vessel detection systems for refugee rubber inflatables," *Remote Sens.*, vol. 13, no. 8, Apr. 2021, Art. no. 1487, doi: 10.3390/rs13081487.

[8] Y. Song, J. Li, P. Gao, L. Li, T. Tian, and J. Tian, "Two-stage cross-modality transfer learning method for military-civilian SAR ship recognition," *IEEE Geosci. Remote Sens. Lett.*, vol. 19, 2022, Art. no. 4506405, doi: 10.1109/LGRS.2022.3162707.

[9] *Review of Maritime Transport: Navigating Stormy Waters* (United Nations Conf. Trade Develop.). Geneva, Switzerland: United Nations, 2022.

[10] E. Schwarz, D. Krause, M. Berg, H. Daedelow, and H. Maass, "Near real time applications for maritime situational awareness," *Int. Arch. Photogramm. Remote Sens. Spatial Inf. Sci.*, vol. XL-7/W3, pp. 999–1003, Apr. 2015, doi: 10.5194/isprsarchives-XL-7-W3-999-2015.

[11] H. Greidanus, M. Alvarez, C. Santamaria, F. Thoorens, N. Kourti, and P. Argentieri, "The SUMO ship detector algorithm for satellite radar images," *Remote Sens.*, vol. 9, no. 3, Mar. 2017, Art. no. 248, doi: 10.3390/rs9030246.

[12] U. Kanjir, H. Greidanus, and K. Oštir, "Vessel detection and classification from spaceborne optical images: A literature survey," *Remote Sens. Environ.*, vol. 207, pp. 1–26, Mar. 2018, doi: 10.1016/j.rse.2017.12.033.

[13] International Maritime Organization, "Resolution A.1106(29) - Guidelines for the onboard operational use of shipborne automatic identification systems (AIS)," 2015. [Online]. Available: https://wwwcdn.imo.org/localresources/en/KnowledgeCentre/IndexofIMOResolutions/AssemblyDocuments/A.1106(29).pdf

[14] European Union Council, *Council Regulation (EC) No 1224/2009*, 2009.

[15] Coast Guard, Department of Homeland Security, *33 CFR 164.46*, 2021. [Online]. Available: https://www.ecfr.gov/current/title-33/part-164/section-164.46

[16] R. Pelich et al., "Large-scale automatic vessel monitoring based on dual-polarization Sentinel-1 and AIS data," *Remote Sens.*, vol. 11, no. 9, May 2019, Art. no. 1078, doi: 10.3390/rs11091078.

[17] B. A. Williams et al., "Global rarity of intact coastal regions," *Conservation Biol.*, vol. 36, no. 4, Aug. 2022, Art. no. e13874, doi: 10.1111/cobi.13874.

[18] D. S. Ilcev, "Space remote sensing and detecting systems of oceangoing ships," *Trans. Maritime Sci.*, vol. 9, no. 2, pp. 187–205, Oct. 2020, doi: 10.7225/toms.v09.n02.004.

[19] F. Fan et al., "Efficient instance segmentation paradigm for interpreting SAR and optical Images," *Remote Sens.*, vol. 14, no. 3, Jan. 2022, Art. no. 531, doi: 10.3390/rs14030531.

[20] Z. Hong et al., "Multi-scale ship detection from SAR and optical imagery via a more accurate YOLOv3," *IEEE J. Sel. Topics Appl. Earth Observ. Remote Sens.*, vol. 14, pp. 6083–6101, 2021, doi: 10.1109/JSTARS.2021.3087555.

[21] M. Reggiannini et al., "Remote sensing for maritime monitoring and vessel prompt identification," in *Cryptology and Network Security*, vol. 11124, J. Camenisch and P. Papadimitratos, Eds., Cham, Switzerland: Springer, 2019, pp. 343–352, Accessed: Dec. 5, 2022. [Online]. Available: http://link.springer.com/10.1007/978-3-319-98678-4_35

[22] C. Xu, X. Zheng, and X. Lu, "Multi-level alignment network for cross-domain ship detection," *Remote Sens.*, vol. 14, no. 10, May 2022, Art. no. 2389, doi: 10.3390/rs14102389.

[23] A. Moreira, P. Prats-Iraola, M. Younis, G. Krieger, I. Hajnsek, and K. P. Papathanassiou, "A tutorial on synthetic aperture radar," *IEEE Geosci. Remote Sens. Mag.*, vol. 1, no. 1, pp. 6–43, Mar. 2013, doi: 10.1109/MGRS.2013.2248301.

[24] R. A. Ryerson, F. M. Henderson, and A. J. Lewis, Eds., *Manual of Remote Sensing*, 3rd. ed. New York, NY, USA: Wiley, 1998.

[25] J. C. Curlander and R. N. MacDonough, *Synthetic Aperture Radar: Systems and Signal Processing* (Wiley Ser. Remote Sensing). New York, NY, USA: Wiley, 1991.

[26] Z. Wang, T. Yang, and H. Zhang, "Land contained sea area ship detection using spaceborne image," *Pattern Recognit. Lett.*, vol. 130, pp. 125–131, Feb. 2020, doi: 10.1016/j.patrec.2019.01.015.

[27] M. Stasolla, J. J. Mallorqui, G. Margarit, C. Santamaria, and N. Walker, "A comparative study of operational vessel detectors for maritime surveillance using satellite-borne synthetic aperture radar," *IEEE J. Sel. Topics Appl. Earth Observ. Remote Sens.*, vol. 9, no. 6, pp. 2687–2701, Jun. 2016, doi: 10.1109/JSTARS.2016.2551730.

[28] J. Li, C. Xu, H. Su, L. Gao, and T. Wang, "Deep learning for SAR ship detection: Past, present, and future," *Remote Sens.*, vol. 14, no. 11, Jun. 2022, Art. no. 2712, doi: 10.3390/rs14112712.

[29] M. Yasir et al., "Ship detection based on deep learning using SAR imagery: A systematic literature review," *Soft Comput.*, vol. 27, pp. 63–84, Oct. 2022, doi: 10.1007/s00500-022-07522-w.

[30] Y. Wang, C. Wang, H. Zhang, Y. Dong, and S. Wei, "A SAR dataset of ship detection for deep learning under complex backgrounds," *Remote Sens.*, vol. 11, no. 7, Mar. 2019, Art. no. 765, doi: 10.3390/rs11070765.

[31] L. Huang et al., "OpenSARShip: A dataset dedicated to Sentinel-1 ship interpretation," *IEEE J. Sel. Topics Appl. Earth Observ. Remote Sens.*, vol. 11, no. 1, pp. 195–208, Jan. 2018, doi: 10.1109/JSTARS.2017.2755672.

[32] B. Li, B. Liu, L. Huang, W. Guo, Z. Zhang, and W. Yu, "OpenSARShip 2.0: A large-volume dataset for deeper interpretation of ship targets in Sentinel-1 imagery," in *Proc. SAR Big Data Era: Models, Methods Appl.*, Beijing, China: IEEE, Nov. 2017, pp. 1–5, doi: 10.1109/BIGSARDATA.2017.8124929.

[33] T. Zhang et al., "LS-SSDD-v1.0: A deep learning dataset dedicated to small ship detection from large-scale Sentinel-1 SAR images," *Remote Sens.*, vol. 12, no. 18, Sep. 2020, Art. no. 2997, doi: 10.3390/rs12182997.

[34] T. Zhang et al., "SAR ship detection dataset (SSDD): Official release and comprehensive data analysis," *Remote Sens.*, vol. 13, no. 18, Sep. 2021, Art. no. 3690, doi: 10.3390/rs13183690.

[35] M. J. Page et al., "The PRISMA 2020 statement: An updated guideline for reporting systematic reviews," *Syst. Rev.*, vol. 10, no. 1, Dec. 2021, Art. no. 89, doi: 10.1186/s13643-021-01626-4.

[36] M. Gusenbauer and N. R. Haddaway, "Which academic search systems are suitable for systematic reviews or meta-analyses? Evaluating retrieval qualities of google scholar, PubMed, and 26 other resources," *Res. Synth. Methods*, vol. 11, no. 2, pp. 181–217, Mar. 2020, doi: 10.1002/jrsm.1378.

[37] M. Aria and C. Cuccurullo, "bibliometrix : An R-tool for comprehensive science mapping analysis," *J. Informetrics*, vol. 11, no. 4, pp. 959–975, Nov. 2017, doi: 10.1016/j.joi.2017.08.007.

[38] L. Lin, Z. Jixian, L. Wanwu, and S. Qiaoli, "Marine target extraction based on adjoint covariance correction model," *Radio Sci.*, vol. 57, no. 3, Mar. 2022, Art. no. e2020RS007233, doi: 10.1029/2020RS007233.

[39] M. Li, X. Cui, and S. Chen, "Adaptive superpixel-level CFAR detector for SAR inshore dense ship detection," *IEEE Geosci. Remote Sens. Lett.*, vol. 19, 2022, Art. no. 4010405, 2022, doi: 10.1109/LGRS.2021.3059253.

[40] S. Wang, M. Wang, S. Yang, and L. Jiao, "New hierarchical saliency filtering for fast ship detection in high-resolution SAR images," *IEEE Trans. Geosci. Remote Sens.*, vol. 55, no. 1, pp. 351–362, Jan. 2017, doi: 10.1109/TGRS.2016.2606481.

[41] S. Tian, C. Wang, and H. Zhang, "Ship detection method for single-polarization synthetic aperture radar imagery based on target enhancement and nonparametric clutter estimation," *J. Appl. Remote Sens.*, vol. 9, no. 1, Mar. 2015, Art. no. 096073, doi: 10.1117/1.JRS.9.096073.

[42] K. Ji, X. Xing, H. Zou, and J. Sun, "A novel variable index and excision CFAR based ship detection method on SAR imagery," *J. Sensors*, vol. 2015, pp. 1–10, 2015, doi: 10.1155/2015/437083.

[43] N. Liu, Z. Cao, Z. Cui, Y. Pi, and S. Dang, "Multi-scale proposal generation for ship detection in SAR images," *Remote Sens.*, vol. 11, no. 5, Mar. 2019, Art. no. 526, doi: 10.3390/rs11050526.

[44] L. Zhang, Z. Zhang, S. Lu, D. Xiang, and Y. Su, "Fast superpixel-based non-window CFAR ship detector for SAR imagery," *Remote Sens.*, vol. 14, no. 9, Apr. 2022, Art. no. 2092, doi: 10.3390/rs14092092.

[45] G. Shu, J. Chang, J. Lu, Q. Wang, and N. Li, "A novel method for SAR ship detection based on eigensubspace projection," *Remote Sens.*, vol. 14, no. 14, Jul. 2022, Art. no. 3441, doi: 10.3390/rs14143441.

[46] C. Santamaria, M. Alvarez, H. Greidanus, V. Syrris, P. Soille, and P. Argentieri, "Mass processing of Sentinel-1 images for maritime surveillance," *Remote Sens.*, vol. 9, no. 7, Jul. 2017, Art. no. 678, doi: 10.3390/rs9070678.

[47] X. Leng, K. Ji, S. Zhou, X. Xing, and H. Zou, "An adaptive ship detection scheme for spaceborne SAR imagery," *Sensors*, vol. 16, no. 9, Aug. 2016, Art. no. 1345, doi: 10.3390/s16091345.

[48] N. Li, X. Pan, L. Yang, Z. Huang, Z. Wu, and G. Zheng, "Adaptive CFAR method for SAR ship detection using intensity and texture feature fusion attention contrast mechanism," *Sensors*, vol. 22, no. 21, Oct. 2022, Art. no. 8116, doi: 10.3390/s22218116.

[49] K.-A. Park, J.-J. Park, J.-C. Jang, J.-H. Lee, S. Oh, and M. Lee, "Multi-spectral ship detection using optical, hyperspectral, and microwave SAR remote sensing data in coastal regions," *Sustainability*, vol. 10, no. 11, Nov. 2018, Art. no. 4064, doi: 10.3390/su10114064.

[50] A. Grover, S. Kumar, and A. Kumar, "Ship detection using Sentinel-1 SAR data," in *Proc. ISPRS Ann. Photogrammetry, Remote Sens. Spatial Inf. Sci.*, Nov. 2018, pp. 317–324, doi: 10.5194/isprs-annals-IV-5-317-2018.

[51] C. Theoharatos, A. Makedonas, N. Fragoulis, V. Tsagaris, and S. Costicoglou, "Detection of ship targets in polarimetric SAR data using 2D-PCA data fusion," *Int. Arch. Photogramm. Remote Sens. Spatial Inf. Sci.*, vol. XL-7/W3, pp. 1017–1024, Apr. 2015, doi: 10.5194/isprsarchives-XL-7-W3-1017-2015.

[52] R.-M. Pelich et al., "Vessel monitoring in the North Sea and Baltic Sea areas based on dual-polarization SAR images and AIS data," in *Proc. Int. Astronaut. Congr. (IAC)*, Bremen, Germany, 2018.

[53] J. Ai et al., "Robust CFAR ship detector based on bilateral-trimmed-statistics of complex ocean scenes in SAR imagery: A closed-form solution," *IEEE Trans. Aerosp. Electron. Syst.*, vol. 57, no. 3, pp. 1872–1890, Jun. 2021, doi: 10.1109/TAES.2021.3050654.

[54] H. Li, X. Cui, and S. Chen, "PolSAR ship detection with optimal polarimetric rotation domain features and SVM," *Remote Sens.*, vol. 13, no. 19, Sep. 2021, Art. no. 3932, doi: 10.3390/rs13193932.

[55] H. Mahgoun, N. E. Chaffa, M. Ouarzeddine, and B. Souissi, "Application of polarimetric-SAR decompositions on RADARSAT-2 fine quad-pol images to enhance the performances of ships detection algorithms," *Sens. Imag.*, vol. 21, no. 1, Dec. 2020, Art. no. 56, doi: 10.1007/s11220-020-00321-3.

[56] T. Zhang, Z. Yang, and H. Xiong, "PolSAR ship detection based on the polarimetric covariance difference matrix," *IEEE J. Sel. Topics Appl. Earth Observ. Remote Sens.*, vol. 10, no. 7, pp. 3348–3359, Jul. 2017, doi: 10.1109/JSTARS.2017.2671904.

[57] Z. Xu, C. Fan, S. Cheng, J. Wang, and X. Huang, "A distribution independent ship detector for PolSAR images," *IEEE J. Sel. Topics Appl. Earth Observ. Remote Sens.*, vol. 14, pp. 3774–3786, 2021, doi: 10.1109/JSTARS.2021.3068843.

[58] X. Cui, C. Tao, Y. Su, and S. Chen, "PolSAR ship detection based on polarimetric correlation pattern," *IEEE Geosci. Remote Sens. Lett.*, vol. 18, no. 3, pp. 471–475, Mar. 2021, doi: 10.1109/LGRS.2020.2976477.

[59] H. Lin, H. Wang, J. Wang, J. Yin, and J. Yang, "A novel ship detection method via generalized polarization relative entropy for PolSAR images," *IEEE Geosci. Remote Sens. Lett.*, vol. 19, 2022, Art. no. 4001205, doi: 10.1109/LGRS.2020.3019196.

[60] C. Zhang, H. Zhang, C. Wang, Q. Fu, and L. Xu, "A novel ship detection method based on Shannon entropy in Chinese Gaofen-3 fully polarimetric SAR images," in *Proc. Prog. Electromagnetics Res. Symp. - Fall*, Nov. 2017, pp. 909–916, doi: 10.1109/PIERS-FALL.2017.8293263.

[61] A. Marino and I. Hajnsek, "Statistical tests for a ship detector based on the polarimetric notch filter," *IEEE Trans. Geosci. Remote Sens.*, vol. 53, no. 8, pp. 4578–4595, Aug. 2015, doi: 10.1109/TGRS.2015.2402312.

[62] R. Touzi, J. Hurley, and P. W. Vachon, "Optimization of the degree of polarization for enhanced ship detection using polarimetric RADARSAT-2," *IEEE Trans. Geosci. Remote Sens.*, vol. 53, no. 10, pp. 5403–5424, Oct. 2015, doi: 10.1109/TGRS.2015.2422134.

[63] T. Zhang, A. Marino, H. Xiong, and W. Yu, "A ship detector applying principal component analysis to the polarimetric notch filter," *Remote Sens.*, vol. 10, no. 6, Jun. 2018, Art. no. 948, doi: 10.3390/rs10060948.

[64] H. Lin, H. Chen, H. Wang, J. Yin, and J. Yang, "Ship detection for PolSAR images via task-driven discriminative dictionary learning," *Remote Sens.*, vol. 11, no. 7, Mar. 2019, Art. no. 769, doi: 10.3390/rs11070769.

[65] M. Gu, Y. Wang, H. Liu, and P. Wang, "PolSAR ship detection based on a SIFT-like PolSAR keypoint detector," *Remote Sens.*, vol. 14, no. 12, Jun. 2022, Art. no. 2900, doi: 10.3390/rs14122900.

[66] C. Schwegmann, W. Kleynhans, and B. Salmon, "Synthetic aperture radar ship detection using Haar-like features," *IEEE Geosci. Remote Sens. Lett.*, vol. 14, no. 2, pp. 154–158, Feb. 2017, doi: 10.1109/LGRS.2016.2631638.

[67] G. He et al., "An adaptive ship detection algorithm for HRWS SAR images under complex background: Application to Sentinel-1 data," *Int. Arch. Photogramm. Remote Sens. Spatial Inf. Sci.*, vol. XLII–3, pp. 497–503, Apr. 2018, doi: 10.5194/isprs-archives-XLII-3-497-2018.

[68] M. C. Proença and J. M. Marques, "Maritime traffic surveillance with SENTINEL-1 high resolution images," *WSEAS Trans. Environ. Develop.*, vol. 14, pp. 501–507, 2018.

[69] X. Leng, K. Ji, S. Zhou, and X. Xing, "Ship detection based on complex signal kurtosis in single-channel SAR imagery," *IEEE Trans. Geosci. Remote Sens.*, vol. 57, no. 9, pp. 6447–6461, Sep. 2019, doi: 10.1109/TGRS.2019.2906054.

[70] Y. Xu, W. Xiong, Y. Lv, and H. Liu, "A new method based on two-stage detection mechanism for detecting ships in high-resolution SAR images," *MATEC Web Conf.*, vol. 128, 2017, Art. no. 01014, doi: 10.1051/matecconf/201712801014.

[71] J. Ai, R. Tian, Q. Luo, J. Jin, and B. Tang, "Multi-scale rotation-invariant Haar-like feature integrated CNN-based ship detection algorithm of multiple-target environment in SAR imagery," *IEEE Trans. Geosci. Remote Sens.*, vol. 57, no. 12, pp. 10070–10087, Dec. 2019, doi: 10.1109/TGRS.2019.2931308.

[72] X. Wang, G. Li, X.-P. Zhang, and Y. He, "Ship detection in SAR images via local contrast of fisher vectors," *IEEE Trans. Geosci. Remote Sens.*, vol. 58, no. 9, pp. 6467–6479, Sep. 2020, doi: 10.1109/TGRS.2020.2976880.

[73] W. Huo, Y. Huang, J. Pei, Q. Zhang, Q. Gu, and J. Yang, "Ship detection from ocean SAR image based on local contrast variance weighted information entropy," *Sensors*, vol. 18, no. 4, Apr. 2018, Art. no. 1196, doi: 10.3390/s18041196.

[74] X. Cong-An et al., "Feature aligned ship detection based on improved RPDet in SAR images," *Displays*, vol. 74, Sep. 2022, Art. no. 102191, doi: 10.1016/j.displa.2022.102191.

[75] T. Zhang, X. Zhang, J. Shi, and S. Wei, "HyperLi-Net: A hyper-light deep learning network for high-accurate and high-speed ship detection from synthetic aperture radar imagery," *ISPRS J. Photogrammetry Remote Sens.*, vol. 167, pp. 123–153, Sep. 2020, doi: 10.1016/j.isprsjprs.2020.05.016.

[76] T. Zhang et al., "Balance learning for ship detection from synthetic aperture radar remote sensing imagery," *ISPRS J. Photogrammetry Remote Sens.*, vol. 182, pp. 190–207, Dec. 2021, doi: 10.1016/j.isprsjprs.2021.10.010.

[77] K. Zhao, Y. Zhou, X. Chen, B. Wang, and Y. Zhang, "Ship detection from scratch in synthetic aperture radar (SAR) images," *Int. J. Remote Sens.*, vol. 42, no. 13, pp. 5010–5024, Jul. 2021, doi: 10.1080/01431161.2021.1906980.

[78] A. Raj J, S. M. Idicula, and B. Paul, "Lightweight SAR Ship detection and 16 class classification using novel deep learning algorithm with a hybrid preprocessing technique," *Int. J. Remote Sens.*, vol. 43, no. 15/16, pp. 5820–5847, Aug. 2022, doi: 10.1080/01431161.2021.2008544.

[79] J. Zhao, Z. Zhang, W. Yu, and T. Truong, "A cascade coupled convolutional neural network guided visual attention method for ship detection from SAR images," *IEEE Access*, vol. 6, pp. 50693–50708, 2018, doi: 10.1109/ACCESS.2018.2869289.

[80] Y. Mao, Y. Yang, Z. Ma, M. Li, H. Su, and J. Zhang, "Efficient low-cost ship detection for SAR imagery based on simplified U-Net," *IEEE Access*, vol. 8, pp. 69742–69753, 2020, doi: 10.1109/ACCESS.2020.2985637.

[81] R. Wang, S. Shao, M. An, J. Li, S. Wang, and X. Xu, "Soft thresholding attention network for adaptive feature denoising in SAR ship detection," *IEEE Access*, vol. 9, pp. 29090–29105, 2021, doi: 10.1109/ACCESS.2021.3059033.

[82] D. Kumar and X. Zhang, "Ship detection based on faster R-CNN in SAR imagery by anchor box optimization," in *Proc. Int. Conf. Control, Automat. Inf. Sci.*, Chengdu, China: IEEE, Oct. 2019, pp. 1–6, doi: 10.1109/ICCAIS46528.2019.9074690.

[83] S. Hou, X. Ma, X. Wang, Z. Fu, J. Wang, and H. Wang, "SAR image ship detection based on scene interpretation," in *Proc. IEEE Int. Geosci. Remote Sens. Symp.*, Waikoloa, HI, USA: IEEE, Sep. 2020, pp. 2863–2866, doi: 10.1109/IGARSS39084.2020.9323473.

[84] C. Zhu, D. Zhao, Z. Liu, and Y. Mao, "Hierarchical attention for ship detection in SAR images," in *Proc. IEEE Int. Geosci. Remote Sens. Symp.*, Waikoloa, HI, USA: IEEE, Sep. 2020, pp. 2145–2148, doi: 10.1109/IGARSS39084.2020.9324122.

[85] N. Ferreira and M. Silveira, "Ship detection in SAR images using convolutional variational autoencoders," in *Proc IEEE Int. Geosci. Remote Sens. Symp.*, Waikoloa, HI, USA: IEEE, Sep. 2020, pp. 2503–2506, doi: 10.1109/IGARSS39084.2020.9324389.

[86] Y. Zhao, L. Zhao, B. Xiong, and G. Kuang, "Attention receptive pyramid network for ship detection in SAR images," *IEEE J. Sel. Topics Appl. Earth Observ. Remote Sens.*, vol. 13, pp. 2738–2756, 2020, doi: 10.1109/JSTARS.2020.2997081.

[87] Y. He, F. Gao, J. Wang, A. Hussain, E. Yang, and H. Zhou, "Learning polar encodings for arbitrary-oriented ship detection in SAR images," *IEEE J. Sel. Topics Appl. Earth Observ. Remote Sens.*, vol. 14, pp. 3846–3859, 2021, doi: 10.1109/JSTARS.2021.3068530.

[88] T. Zhang et al., "Balance scene learning mechanism for offshore and inshore ship detection in SAR images," *IEEE Geosci. Remote Sens. Lett.*, vol. 19, 2022, Art. no. 4004905, doi: 10.1109/LGRS.2020.3033988.

[89] Z. Deng, H. Sun, S. Zhou, and J. Zhao, "Learning deep ship detector in SAR images from scratch," *IEEE Trans. Geosci. Remote Sens.*, vol. 57, no. 6, pp. 4021–4039, Jun. 2019, doi: 10.1109/TGRS.2018.2889353.

[90] Z. Cui, Q. Li, Z. Cao, and N. Liu, "Dense attention pyramid networks for multi-scale ship detection in SAR images," *IEEE Trans. Geosci. Remote Sens.*, vol. 57, no. 11, pp. 8983–8997, Nov. 2019, doi: 10.1109/TGRS.2019.2923988.

[91] S. Wei, X. Zeng, H. Zhang, Z. Zhou, J. Shi, and X. Zhang, "LFG-Net: Low-level feature guided network for precise ship instance segmentation in SAR images," *IEEE Trans. Geosci. Remote Sens.*, vol. 60, 2022, Art. no. 5231017, doi: 10.1109/TGRS.2022.3188677.

[92] P. Zhang, G. Xie, and J. Zhang, "Gaussian function fusing fully convolutional network and region proposal-based network for ship target detection in SAR images," *Int. J. Antennas Propag.*, vol. 2022, pp. 1–20, May 2022, doi: 10.1155/2022/3063965.

[93] P. Chen, Y. Li, H. Zhou, B. Liu, and P. Liu, "Detection of small ship objects using anchor boxes cluster and feature pyramid network model for SAR imagery," *JMSE*, vol. 8, no. 2, Feb. 2020, Art. no. 112, doi: 10.3390/jmse8020112.

[94] F. Gao, W. Shi, J. Wang, E. Yang, and H. Zhou, "Enhanced feature extraction for ship detection from multi-resolution and multi-scene synthetic aperture radar (SAR) images," *Remote Sens.*, vol. 11, no. 22, Nov. 2019, Art. no. 2694, doi: 10.3390/rs11222694.

[95] C. Dechesne, S. Lefevre, R. Vadaine, G. Hajduch, and R. Fablet, "Ship identification and characterization in Sentinel-1 SAR images with multi-task deep learning," *Remote Sens.*, vol. 11, no. 24, Dec. 2019, Art. no. 2997, doi: 10.3390/rs11242997.

[96] S. Chen, J. Zhang, and R. Zhan, "R2FA-Det: Delving into high-quality rotatable boxes for ship detection in SAR images," *Remote Sens.*, vol. 12, no. 12, Jun. 2020, Art. no. 2031, doi: 10.3390/rs12122031.

[97] L. Tian, Y. Cao, B. He, Y. Zhang, C. He, and D. Li, "Image enhancement driven by object characteristics and dense feature reuse network for ship target detection in remote sensing imagery," *Remote Sens.*, vol. 13, no. 7, Mar. 2021, Art. no. 1327, doi: 10.3390/rs13071327.

[98] T. Zhang, X. Zhang, and X. Ke, "Quad-FPN: A novel quad feature pyramid network for SAR ship detection," *Remote Sens.*, vol. 13, no. 14, Jul. 2021, Art. no. 2771, doi: 10.3390/rs13142771.

[99] D. Zhao, C. Zhu, J. Qi, X. Qi, Z. Su, and Z. Shi, "Synergistic attention for ship instance segmentation in SAR images," *Remote Sens.*, vol. 13, no. 21, Oct. 2021, Art. no. 4384, doi: 10.3390/rs13214384.

[100] N. Su, J. He, Y. Yan, C. Zhao, and X. Xing, "SII-Net: Spatial information integration network for small target detection in SAR images," *Remote Sens.*, vol. 14, no. 3, Jan. 2022, Art. no. 442, doi: 10.3390/rs14030442.

[101] R. Xia et al., "CRTransSar: A visual transformer based on contextual joint representation learning for SAR ship detection," *Remote Sens.*, vol. 14, no. 6, Mar. 2022, Art. no. 1488, doi: 10.3390/rs14061488.

[102] B. He, Q. Zhang, M. Tong, and C. He, "Oriented ship detector for remote sensing imagery based on pairwise branch detection head and SAR feature enhancement," *Remote Sens.*, vol. 14, no. 9, May 2022, Art. no. 2177, doi: 10.3390/rs14092177.

[103] K. Li, M. Zhang, M. Xu, R. Tang, L. Wang, and H. Wang, "Ship detection in SAR images based on feature enhancement Swin transformer and adjacent feature fusion," *Remote Sens.*, vol. 14, no. 13, Jul. 2022, Art. no. 3186, doi: 10.3390/rs14133186.

[104] X. Li, D. Li, H. Liu, J. Wan, Z. Chen, and Q. Liu, "A-BFPN: An attention-guided balanced feature pyramid network for SAR ship detection," *Remote Sens.*, vol. 14, no. 15, Aug. 2022, Art. no. 3829, doi: 10.3390/rs14153829.

[105] Z. Xu, R. Gao, K. Huang, and Q. Xu, "Triangle distance IoU loss, attention-weighted feature pyramid network, and rotated-SARShip dataset for arbitrary-oriented SAR ship detection," *Remote Sens.*, vol. 14, no. 18, Sep. 2022, Art. no. 4676, doi: 10.3390/rs14184676.

[106] G. Yan, Z. Chen, Y. Wang, Y. Cai, and S. Shuai, "LssDet: A lightweight deep learning detector for SAR ship detection in high-resolution SAR images," *Remote Sens.*, vol. 14, no. 20, Oct. 2022, Art. no. 5148, doi: 10.3390/rs14205148.

[107] L. Zhang et al., "Filtered convolution for synthetic aperture radar images ship detection," *Remote Sens.*, vol. 14, no. 20, Oct. 2022, Art. no. 5257, doi: 10.3390/rs14205257.

[108] X. Xu et al., "A group-wise feature enhancement-and-fusion network with dual-polarization feature enrichment for SAR ship detection," *Remote Sens.*, vol. 14, no. 20, Oct. 2022, Art. no. 5276, doi: 10.3390/rs14205276.

[109] Z. Zhou, Z. Cui, Z. Zang, X. Meng, Z. Cao, and J. Yang, "UltraHi-PrNet: An ultra-high precision deep learning network for dense multi-scale target detection in SAR images," *Remote Sens.*, vol. 14, no. 21, Nov. 2022, Art. no. 5596, doi: 10.3390/rs14215596.

[110] M. Kang, K. Ji, X. Leng, and Z. Lin, "Contextual region-based convolutional neural network with multilayer fusion for SAR ship detection," *Remote Sens.*, vol. 9, no. 8, Aug. 2017, Art. no. 860, doi: 10.3390/rs9080860.

[111] Y. Gui, X. Li, and L. Xue, "A multilayer fusion light-head detector for SAR ship detection," *Sensors*, vol. 19, no. 5, Mar. 2019, Art. no. 1124, doi: 10.3390/s19051124.

[112] Z. Pan, R. Yang, and Z. Zhang, "MSR2N: Multi-stage rotational region based network for arbitrary-oriented ship detection in SAR images," *Sensors*, vol. 20, no. 8, Apr. 2020, Art. no. 2340, doi: 10.3390/s20082340.

[113] W. Dai, Y. Mao, R. Yuan, Y. Liu, X. Pu, and C. Li, "A novel detector based on convolution neural networks for multiscale SAR ship detection in complex background," *Sensors*, vol. 20, no. 9, Apr. 2020, Art. no. 2547, doi: 10.3390/s20092547.

[114] H. Zhu, Y. Xie, H. Huang, C. Jing, Y. Rong, and C. Wang, "DB-YOLO: A duplicate bilateral YOLO network for multi-scale ship detection in SAR images," *Sensors*, vol. 21, no. 23, Dec. 2021, Art. no. 8146, doi: 10.3390/s21238146.

[115] M. A. Elshafey, "Towards a reliable and sensitive deep learning based approach for multi-ship detection in SAR imagery," *IJG*, no. 17, pp. 59–70, Dec. 2021, doi: 10.52939/ijg.v17i6.2067.

[116] K. Ding et al., "Towards real-time detection of ships and wakes with lightweight deep learning model in Gaofen-3 SAR images," *Remote Sens. Environ.*, vol. 284, Jan. 2023, Art. no. 113345, doi: 10.1016/j.rse.2022.113345.

[117] Z. Wang, B. Wang, and N. Xu, "SAR ship detection in complex background based on multi-feature fusion and non-local channel attention mechanism," *Int. J. Remote Sens.*, vol. 42, no. 19, pp. 7519–7550, Oct. 2021, doi: 10.1080/01431161.2021.1963003.

[118] Y. Wang, C. Wang, and H. Zhang, "Combining a single shot multibox detector with transfer learning for ship detection using sentinel-1 SAR images," *Remote Sens. Lett.*, vol. 9, no. 8, pp. 780–788, 2018, doi: 10.1080/2150704X.2018.1475770.

[119] J. Wang, Y. Lin, J. Guo, and L. Zhuang, "SSS-YOLO: Towards more accurate detection for small ships in SAR image," *Remote Sens. Lett.*, vol. 12, no. 2, pp. 122–131, Feb. 2021, doi: 10.1080/2150704X.2020.1837988.

[120] X. Zhang et al., "A lightweight feature optimizing network for ship detection in SAR image," *IEEE Access*, vol. 7, pp. 141662–141678, 2019, doi: 10.1109/ACCESS.2019.2943241.

[121] C. Chen, C. He, C. Hu, H. Pei, and L. Jiao, "MSARN: A deep neural network based on an adaptive recalibration mechanism for multi-scale and arbitrary-oriented SAR ship detection," *IEEE Access*, vol. 7, pp. 159262–159283, 2019, doi: 10.1109/ACCESS.2019.2951030.

[122] L. Han, D. Ran, W. Ye, W. Yang, and X. Wu, "Multi-size convolution and learning deep network for SAR ship detection from scratch," *IEEE Access*, vol. 8, pp. 158996–159016, 2020, doi: 10.1109/ACCESS.2020.3020363.

[123] G. Zhang, Z. Li, X. Li, C. Yin, and Z. Shi, "A novel salient feature fusion method for ship detection in synthetic aperture radar images," *IEEE Access*, vol. 8, pp. 215904–215914, 2020, doi: 10.1109/ACCESS.2020.3041372.

[124] H. Su, S. Wei, M. Wang, L. Zhou, J. Shi, and X. Zhang, "Ship detection based on RetinaNet-plus for high-resolution SAR imagery," in *Proc. 6th Asia-Pac. Conf. Synthetic Aperture Radar*, Xiamen, China: IEEE, Nov. 2019, pp. 1–5, doi: 10.1109/APSAR46974.2019.9048269.

[125] T. Zhang, X. Zhang, J. Shi, and S. Wei, "High-speed ship detection in SAR images by improved Yolov3," in *Proc.16th Int. Comput. Conf. Wavelet Act. Media Technol. Inf. Process.*, Chengdu, China: IEEE, Dec. 2019, pp. 149–152, doi: 10.1109/ICCWAMTIP47768.2019.9067695.

[126] L. Han, W. Ye, J. Li, and D. Ran, "Small ship detection in SAR images based on modified SSD," in *Proc. IEEE Int. Conf. Signal, Inf. Data Process.*, Chongqing, China: IEEE, Dec. 2019, pp. 1–5, doi: 10.1109/ICSIDP47821.2019.9173268.

[127] Y. Wang, C. Wang, and H. Zhang, "Ship discrimination with deep convolutional neural networks in SAR images," in *Proc. IEEE Int. Geosci. Remote Sens. Symp.*, Valencia, Spain: IEEE, Jul. 2018, pp. 8444–8447, doi: 10.1109/IGARSS.2018.8519552.

[128] S. Chen, R. Zhan, W. Wang, and J. Zhang, "Learning slimming SAR ship object detector through network pruning and knowledge distillation," *IEEE J. Sel. Topics Appl. Earth Observ. Remote Sens.*, vol. 14, pp. 1267–1282, 2021, doi: 10.1109/JSTARS.2020.3041783.

[129] R. Yang, Z. Pan, X. Jia, L. Zhang, and Y. Deng, "A novel CNN-based detector for ship detection based on rotatable bounding box in SAR images," *IEEE J. Sel. Topics Appl. Earth Observ. Remote Sens.*, vol. 14, pp. 1938–1958, 2021, doi: 10.1109/JSTARS.2021.3049851.

[130] Y. Chen, T. Duan, C. Wang, Y. Zhang, and M. Huang, "End-to-end ship detection in SAR images for complex scenes based on deep CNNs," *J. Sensors*, vol. 2021, pp. 1–19, Mar. 2021, doi: 10.1155/2021/8893182.

[131] C. Li et al., "Efficient object detection in SAR images based on computation-aware neural architecture search," *Appl. Sci.*, vol. 12, no. 21, Oct. 2022, Art. no. 10978, doi: 10.3390/app122110978.

[132] S. Jiang and X. Zhou, "DWSC-YOLO: A lightweight ship detector of SAR images based on deep learning," *JMSE*, vol. 10, no. 11, Nov. 2022, Art. no. 1699, doi: 10.3390/jmse10111699.

[133] Y.-L. Chang, A. Anagaw, L. Chang, Y. Wang, C.-Y. Hsiao, and W.-H. Lee, "Ship detection based on YOLOv2 for SAR imagery," *Remote Sens.*, vol. 11, no. 7, Apr. 2019, Art. no. 786, doi: 10.3390/rs11070786.

[134] T. Zhang and X. Zhang, "High-speed ship detection in SAR images based on a grid convolutional neural network," *Remote Sens.*, vol. 11, no. 10, May 2019, Art. no. 1206, doi: 10.3390/rs11101206.

[135] T. Zhang, X. Zhang, J. Shi, and S. Wei, "Depthwise separable convolution neural network for high-speed SAR ship detection," *Remote Sens.*, vol. 11, no. 21, Nov. 2019, Art. no. 2483, doi: 10.3390/rs11212483.

[136] J. Jiang, X. Fu, R. Qin, X. Wang, and Z. Ma, "High-speed lightweight ship detection algorithm based on YOLO-V4 for three-channels RGB SAR image," *Remote Sens.*, vol. 13, no. 10, May 2021, Art. no. 1909, doi: 10.3390/rs13101909.

[137] L. Yu, H. Wu, Z. Zhong, L. Zheng, Q. Deng, and H. Hu, "TWC-Net: A SAR ship detection using two-way convolution and multiscale feature mapping," *Remote Sens.*, vol. 13, no. 13, Jun. 2021, Art. no. 2558, doi: 10.3390/rs13132558.

[138] K. Sun, Y. Liang, X. Ma, Y. Huai, and M. Xing, "DSDet: A lightweight densely connected sparsely activated detector for ship target detection in high-resolution SAR images," *Remote Sens.*, vol. 13, no. 14, Jul. 2021, Art. no. 2743, doi: 10.3390/rs13142743.

[139] Z. Sun, X. Leng, Y. Lei, B. Xiong, K. Ji, and G. Kuang, "BiFA-YOLO: A novel YOLO-based method for arbitrary-oriented ship detection in high-resolution SAR images," *Remote Sens.*, vol. 13, no. 21, Oct. 2021, Art. no. 4209, doi: 10.3390/rs13214209.

[140] J. Yu, G. Zhou, S. Zhou, and M. Qin, "A fast and lightweight detection network for multi-scale SAR ship detection under complex backgrounds," *Remote Sens.*, vol. 14, no. 1, Dec. 2021, Art. no. 31, doi: 10.3390/rs14010031.

[141] X. Xu, X. Zhang, and T. Zhang, "Lite-YOLOv5: A lightweight deep learning detector for on-board ship detection in large-scene Sentinel-1 SAR images," *Remote Sens.*, vol. 14, no. 4, Feb. 2022, Art. no. 1018, doi: 10.3390/rs14041018.

[142] H. Shi, Z. Fang, Y. Wang, and L. Chen, "An adaptive sample assignment strategy based on feature enhancement for ship detection in SAR images," *Remote Sens.*, vol. 14, no. 9, May 2022, Art. no. 2238, doi: 10.3390/rs14092238.

[143] W. Yu, Z. Wang, J. Li, Y. Luo, and Z. Yu, "A lightweight network based on one-level feature for ship detection in SAR images," *Remote Sens.*, vol. 14, no. 14, Jul. 2022, Art. no. 3321, doi: 10.3390/rs14143321.

[144] Z. Shao, X. Zhang, T. Zhang, X. Xu, and T. Zeng, "RBFA-Net: A rotated balanced feature-aligned network for rotated SAR ship detection and classification," *Remote Sens.*, vol. 14, no. 14, Jul. 2022, Art. no. 3345, doi: 10.3390/rs14143345.

[145] J. Yu, T. Wu, S. Zhou, H. Pan, X. Zhang, and W. Zhang, "An SAR ship object detection algorithm based on feature information efficient representation network," *Remote Sens.*, vol. 14, no. 14, Jul. 2022, Art. no. 3489, doi: 10.3390/rs14143489.

[146] S. Li, X. Fu, and J. Dong, "Improved ship detection algorithm based on YOLOX for SAR outline enhancement image," *Remote Sens.*, vol. 14, no. 16, Aug. 2022, Art. no. 4070, doi: 10.3390/rs14164070.

[147] Y. Guo and L. Zhou, "MEA-Net: A lightweight SAR ship detection model for imbalanced datasets," *Remote Sens.*, vol. 14, no. 18, Sep. 2022, Art. no. 4438, doi: 10.3390/rs14184438.

[148] Y. Guo, S. Chen, R. Zhan, W. Wang, and J. Zhang, "LMSD-YOLO: A lightweight YOLO algorithm for multi-scale SAR ship detection," *Remote Sens.*, vol. 14, no. 19, Sep. 2022, Art. no. 4801, doi: 10.3390/rs14194801.

[149] G. Tang, H. Zhao, C. Claramunt, and S. Men, "FLNet: A near-shore ship detection method based on image enhancement technology," *Remote Sens.*, vol. 14, no. 19, Sep. 2022, Art. no. 4857, doi: 10.3390/rs14194857.

[150] S. Wang et al., "YOLO-SD: Small ship detection in SAR Images by multi-scale convolution and feature transformer module," *Remote Sens.*, vol. 14, no. 20, Oct. 2022, Art. no. 5268, doi: 10.3390/rs14205268.

[151] J. Wang, C. Lu, and W. Jiang, "Simultaneous ship detection and orientation estimation in SAR images based on attention module and angle regression," *Sensors*, vol. 18, no. 9, Aug. 2018, Art. no. 2851, doi: 10.3390/s18092851.

[152] F. Xie, B. Lin, and Y. Liu, "Research on the coordinate attention mechanism fuse in a YOLOv5 deep learning detector for the SAR ship detection task," *Sensors*, vol. 22, no. 9, Apr. 2022, Art. no. 3370, doi: 10.3390/s22093370.

[153] J. Yu, T. Wu, X. Zhang, and W. Zhang, "An efficient lightweight SAR ship target detection network with improved regression loss function and enhanced feature information expression," *Sensors*, vol. 22, no. 9, Apr. 2022, Art. no. 3447, doi: 10.3390/s22093447.

[154] L. Pang, B. Li, F. Zhang, X. Meng, and L. Zhang, "A lightweight YOLOv5-MNE algorithm for SAR ship detection," *Sensors*, vol. 22, no. 18, Sep. 2022, Art. no. 7088, doi: 10.3390/s22187088.

[155] F. Xie, H. Luo, S. Li, Y. Liu, and B. Lin, "Using clean energy satellites to interpret imagery: A satellite IoT oriented lightweight object detection framework for SAR Ship detection," *Sustainability*, vol. 14, no. 15, Jul. 2022, Art. no. 9277, doi: 10.3390/su14159277.

[156] L. Jin and G. Liu, "An approach on image processing of deep learning based on improved SSD," *Symmetry*, vol. 13, no. 3, Mar. 2021, Art. no. 495, doi: 10.3390/sym13030495.

[157] H. Guo, X. Yang, N. Wang, and X. Gao, "A centerNet++ model for ship detection in SAR images," *Pattern Recognit.*, vol. 112, Apr. 2021, Art. no. 107787, doi: 10.1016/j.patcog.2020.107787.

[158] H. Peng and X. Tan, "Improved YOLOX's anchor-free SAR image ship target detection," *IEEE Access*, vol. 10, pp. 70001–70015, 2022, doi: 10.1109/ACCESS.2022.3188387.

[159] Z. Sun et al., "An anchor-free detection method for ship targets in high-resolution SAR images," *IEEE J. Sel. Topics Appl. Earth Observ. Remote Sens.*, vol. 14, pp. 7799–7816, 2021, doi: 10.1109/JSTARS.2021.3099483.

[160] Z. Cui, X. Wang, N. Liu, Z. Cao, and J. Yang, "Ship detection in large-scale SAR images via spatial shuffle-group enhance attention," *IEEE Trans. Geosci. Remote Sens.*, vol. 59, no. 1, pp. 379–391, Jan. 2021, doi: 10.1109/TGRS.2020.2997200.

[161] Q. Fan et al., "Ship detection using a fully convolutional network with compact polarimetric SAR images," *Remote Sens.*, vol. 11, no. 18, Sep. 2019, Art. no. 2171, doi: 10.3390/rs11182171.

[162] H. Xie, X. Jiang, J. Zhang, J. Chen, G. Wang, and K. Xie, "Lightweight and anchor-free frame detection strategy based on improved CenterNet for multiscale ships in SAR images," *Front. Comput. Sci.*, vol. 4, Nov. 2022, Art. no. 1012755, doi: 10.3389/fcomp.2022.1012755.

[163] B. He, Q. Zhang, M. Tong, and C. He, "An anchor-free method based on adaptive feature encoding and Gaussian-guided sampling optimization for ship detection in SAR imagery," *Remote Sens.*, vol. 14, no. 7, Apr. 2022, Art. no. 1738, doi: 10.3390/rs14071738.
[164] Y. Feng et al., "A lightweight position-enhanced Anchor-free algorithm for SAR ship detection," *Remote Sens.*, vol. 14, no. 8, Apr. 2022, Art. no. 1908, doi: 10.3390/rs14081908.
[165] M. Zhu, G. Hu, S. Li, H. Zhou, S. Wang, and Z. Feng, "A novel anchor-free method based on FCOS + ATSS for ship detection in SAR images," *Remote Sens.*, vol. 14, no. 9, Apr. 2022, Art. no. 2034, doi: 10.3390/rs14092034.
[166] H. Shi, B. Chai, Y. Wang, and L. Chen, "A local-sparse-information-aggregation transformer with explicit contour guidance for SAR ship detection," *Remote Sens.*, vol. 14, no. 20, Oct. 2022, Art. no. 5247, doi: 10.3390/rs14205247.
[167] Y. Jiang, W. Li, and L. Liu, "R-CenterNet+: Anchor-free detector for ship detection in SAR images," *Sensors*, vol. 21, no. 17, Aug. 2021, Art. no. 5693, doi: 10.3390/s21175693.
[168] H. Greidanus, "SUMO," 2017. [Online]. Available: https://github.com/ec-europa/sumo
[169] R. Garg, A. Kumar, N. Bansal, M. Prateek, and S. Kumar, "Semantic segmentation of PolSAR image data using advanced deep learning model," *Sci. Rep.*, vol. 11, no. 1, Jul. 2021, Art. no. 15365, doi: 10.1038/s41598-021-94422-y.
[170] J. Fu, X. Sun, Z. Wang, and K. Fu, "An anchor-free method based on feature balancing and refinement network for multiscale ship detection in SAR images," *IEEE Trans. Geosci. Remote Sens.*, vol. 59, no. 2, pp. 1331–1344, Feb. 2021, doi: 10.1109/TGRS.2020.3005151.
[171] J. Li, C. Qu, and J. Shao, "Ship detection in SAR images based on an improved faster R-CNN," in *Proc. SAR Big Data Era: Models, Methods Appl.*, Beijing, China: IEEE, Nov. 2017, pp. 1–6, doi: 10.1109/BIGSARDATA.2017.8124934.
[172] S. Xian, W. Zhirui, S. Yuanrui, D. Wenhui, Z. Yue, and F. Kun, "AIR-SARShip-1.0: High-resolution SAR ship detection dataset," 2019, doi: 10.12000/JR19097.
[173] S. Wei, X. Zeng, Q. Qu, M. Wang, H. Su, and J. Shi, "HRSID: A high-resolution SAR images dataset for ship detection and instance segmentation," *IEEE Access*, vol. 8, pp. 120234–120254, 2020, doi: 10.1109/ACCESS.2020.3005861.
[174] Y. Hu, Y. Li, and Z. Pan, "A dual-polarimetric SAR ship detection dataset and a memory-augmented autoencoder-based detection method," *Sensors*, vol. 21, no. 24, Dec. 2021, Art. no. 8478, doi: 10.3390/s21248478.
[175] T.-Y. Lin, P. Dollar, R. Girshick, K. He, B. Hariharan, and S. Belongie, "Feature pyramid networks for object detection," in *Proc. IEEE Conf. Comput. Vis. Pattern Recognit.*, Honolulu, HI, USA: IEEE, Jul. 2017, pp. 936–944, doi: 10.1109/CVPR.2017.106.
[176] S. Lei, D. Lu, X. Qiu, and C. Ding, "SRSDD-v1.0: A high-resolution SAR rotation ship detection dataset," *Remote Sens.*, vol. 13, no. 24, Dec. 2021, Art. no. 5104, doi: 10.3390/rs13245104.
[177] I. Pita et al., "SAR satellite imagery reveals the impact of the Covid-19 crisis on ship frequentation in the French Mediterranean waters," *Front. Mar. Sci.*, vol. 9, May 2022, Art. no. 845419, doi: 10.3389/fmars.2022.845419.
[178] N. Aghaei, G. Akbarizadeh, and A. Kosarian, "GreyWolfLSM: An accurate oil spill detection method based on level set method from synthetic aperture radar imagery," *Eur. J. Remote Sens.*, vol. 55, no. 1, pp. 181–198, Dec. 2022, doi: 10.1080/22797254.2022.2037468.
[179] F. Sharifzadeh, G. Akbarizadeh, and Y. Kavian, "Ship classification in SAR images using a new hybrid CNN-MLP classifier," *J. Ind. Soc. Remote Sens.*, vol. 47, no. 4, pp. 551–562, Apr. 2019, doi: 10.1007/s12524-018-0891-y.
[180] G. Akbarizadeh, G. A. Rezai-Rad, and S. B. Shokouhi, "A new region-based active contour model with skewness wavelet energy for segmentation of SAR images," *IEICE Trans. Inf. Syst.*, vol. E93-D, no. 7, pp. 1690–1699, 2010, doi: 10.1587/transinf.E93.D.1690.
[181] D. M. Nunes et al., "Evidence of illegal fishing within the largest Brazilian coastal MPA: Turning a blind eye to the obvious," *Mar. Policy*, vol. 147, Jan. 2023, Art. no. 105324, doi: 10.1016/j.marpol.2022.105324.
[182] E. Sala et al., "Protecting the global ocean for biodiversity, food and climate," *Nature*, vol. 592, no. 7854, pp. 397–402, Apr. 2021, doi: 10.1038/s41586-021-03371-z.

Cyprien Alexandre received the Ph.D. degree in geography from the University of La Reunion, Saint Denis de La Réunion, France, in 2017.

From 2013 to 2017, he was a part of the International Cooperation Center for Agronomic Research and Development, where he conducted his Ph.D. thesis. Since 2019, he has been a Research Engineer with the French National Research Institute for Sustainable Development, Montpellier, France.

Rodolphe Devillers received the Ph.D. degree in geomatics/geographic information sciences from Laval University, Québec, QC, Canada, and the University of Marne-la-Vallée, Marne, France, in 2004.

He is a Senior Research Scientist with the French National Research Institute on Sustainable Development, Montpellier, France, and is a member of the Espace-Dev Research Laboratory. He specializes in geospatial sciences applied to the marine environment, specifically in the areas of marine conservation.

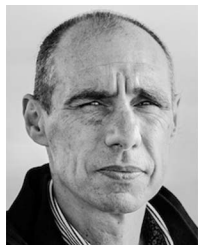

David Mouillot received the Ph.D. degree in ecology and environment from the University of Corsica, Corte, France, in 1999.

He has a background in both ecology and modeling. He runs a research group aiming to increase the interdisciplinary in the study of marine socio-ecosystems under global change. More recently, he contributed to the development of a new generation of tools based on environmental DNA released by all organisms to monitor marine biodiversity and on remote sensing technologies to monitor human activities. He is supported by the Institut Universitaire de France (IUF) and has been a highly cited researcher since 2016.

Raphael Seguin received the master's degree in applied ecology from University of Montpellier, Montpellier, France, in 2022. He is currently working toward the Ph.D. degree in collaboration between the University of Montpellier, Montpellier, France, and the Bloom Association, Paris, France, on the coupling between satellite information and artificial intelligence to better estimate fishing pressure at sea and its carbon cost.

He has contributed to several innovative research projects on conservation linked to marine protected areas and the impact of tourism or the monitoring of maritime traffic from satellite images.

Thibault Catry received the Ph.D. degree in physical modeling for environmental protection from the University of Bologna, Bologna, Italy, in 2011.

He is a Remote Sensing Expert with the French Research Institute for Sustainable Development, UMR Espace-Dev, Montpellier, France. His research interest focuses on the development of methods for processing optical satellite and RADAR images for the characterization of environmental processes.